Kim KT, Levis M, Small D. (2006). Constitutively activated FLT3 phosphorylates BAD partially through pim-1. *Br J Haematol* **134**: 500–509.

Kiyoi H, Naoe T, Yokota S, Nakao M, Minami S, Kuriyama K *et al.* (1997). Internal tandem duplication of FLT3 associated with leukocytosis in acute promyelocytic leukemia. *Leukemia* **11**: 1447–1452.

Konishi Y, Lehtinen M, Donovan N, Bonni A. (2002). Cdc2 phosphorylation of BAD Links the cell cycle to the cell death machinery. *Mol Cell* **9**: 1005–1016.

Levis M, Pham R, Smith BD, Small D. (2004). *In vitro* studies of a FLT3 inhibitor combined with chemotherapy: sequence of administration is important to achieve synergistic cytotoxic effects. *Blood* **104**: 1145–1150.

Levis M, Small D. (2005). FLT3 tyrosine kinase inhibitors. *Int J Hematol* **82**: 100–107.

Lopez-Girona A, Furnari B, Mondesert O, Russell P. (1999). Nuclear localization of Cdc25 is regulated by DNA damage and a14-3-3 protein. *Nature* **397**: 172–175.

Lyman SD, James L, Vanden Bos T, de Vries P, Brasel K, Gliniak B *et al.* (1993). Molecular cloning of a ligand for the flt3/flk-2 tyrosine kinase receptor: a proliferative factor for primitive hematopoietic cells. *Cell* **75**: 1157–1167.

Neben K, Schnittger S, Bross B, Tews B, Kokocinski F, Haferlach T *et al.* (2005). Distinct gene expressions patterns associated with FLT3- and NRAS- activating mutations in acute myeloid leukemia with normal karyotype. *Oncogene* **24**: 1580–1588.

Propper DJ, McDonald AC, Man A, Thavasu P, Balkwill F, Braybrooke JP *et al.* (2001). Phase I and pharmacokinetic study of PKC412, an inhibitor of protein kinase C. *J Clin Oncol* **19**: 1485–1492.

Quentmeier H, Reinhardt J, Zaborski M, Drexler HG. (2003). FLT3 mutations in acute myeloid leukemia cell lines. *Leukemia* **17**: 120–124.

Schmitt E, Beauchemin M, Bertrand R. (2007). Nuclear colocalization and interaction between bcl-xL and cdk1 (cdc2) during G2/M cell-cycle checkpoint. *Oncogene* **26**: 5851–5865.

Small D, Levenstein M, Kim E, Carow C, Amin S, Rockwell P *et al.* (1994). STK-1, the human homolog of Flk-2/Flt-3, is selectively expressed in CD34$^+$ human bone marrow cells and is involved in the proliferation of early progenitor/stem cells. *Proc Natl Acad Sci USA* **91**: 459–463.

Stone RM, DeAngelo DJ, Klimek V, Galinsky I, Estey E, Nimer SD *et al.* (2005). Patients with acute myeloid leukemia and an activating mutation in FLT3 respond to a small-molecule FLT3 tyrosine kinase inhibitor, PKC412. *Blood* **105**: 54–60.

Watanabe N, Broome M, Hunter T. (1995). Regulation of the human Wee1 CDK tyrosine 15 kinase during cell cycle. *EMBO J* **14**: 1878–1891.

Weisberg E, Boulton C, Kelly LM, Manley P, Fabbro D, Meyer T *et al.* (2002). Inhibition of mutant FLT3 receptors in leukemia cells by the small molecule tyrosine kinase inhibitor PKC412. *Cancer Cell* **1**: 433–443.

Yang X, Lui L, Sternberg D, Tang L, Galinsky I, DeAngelo D *et al.* (2005). The FLT3 internal tandem duplication mutation prevents apoptosis in interleukin 3-deprived BaF3 cells due to protein kinase A and ribosomal S6 Kinase 1-mediated BAD phosphorylation at serine 112. *Cancer Res* **65**: 7338–7347.

Yao Q, Nishiuchi R, Li Q, Kumar AR, Hudson WA, Kersey JH. (2003). FLT3 expressing leukemias are selectively sensitive to inhibitors of the molecular chaperone heat shock protein 90 through destabilization of signal transduction-associated kinases. *Clin Cancer Res* **9**: 4483–4493.

Yee KW, Schittenhelm M, O'Farrell AM, Town AR, McGreevey L, Bainbridge T *et al.* (2004). Synergistic effect of SU11248 with cytarabine or daunorubicin on FLT3 ITD-positive leukemic cells. *Blood* **104**: 4202–4209.

Zha J, Harada H, Yang F, Jockel J, Korsmeyer SJ. (1996). Serine phosphorylation of death agonist Bad in response to survival factor results in binding to 14-3-3 not BCL-XL. *Cell* **87**: 619–628.

Supplementary Information accompanies the paper on the Oncogene website (http://www.nature.com/onc).

ORIGINAL ARTICLE

Transcriptional Modulation Using HDACi Depsipeptide Promotes Immune Cell-Mediated Tumor Destruction of Murine B16 Melanoma

Takashi Murakami[1], Atsuko Sato[1,2], Nicole A.L. Chun[1], Mayumi Hara[1], Yuki Naito[1], Yukiko Kobayashi[2,3], Yasuhiko Kano[4], Mamitaro Ohtsuki[2], Yusuke Furukawa[3] and Eiji Kobayashi[1]

With melanoma, as with many other malignancies, aberrant transcriptional repression is a hallmark of refractory cancer. To restore gene expression, use of a histone deacetylase inhibitor (HDACi) is expected to be effective. Our recent DNA micro-array analysis showed that the HDACi depsipeptide (FK228) significantly enhances gp100 antigen expression. Herein, we demonstrate that depsipeptide promotes tumor-specific T-cell-mediated killing of B16/F10 murine melanoma cells. First, by a quantitative assay of caspase-3/7 activity, a sublethal dose of depsipeptide was determined (ED50: 5 nM), in which $p21^{Waf1/Cip1}$ and Fas were sufficiently evoked concomitantly with histone H3 acetylation. Second, the sublethal dose of depsipeptide treatment with either a recombinant Fas ligand or tumor-specific T cells synergistically enhanced apoptotic cell death in B16/F10 cells *in vitro*. Furthermore, we found that depsipeptide increased levels of perforin in T cells. Finally, *in vivo* metastatic growth of B16/F10 in the lung was significantly inhibited by a combination of depsipeptide treatment and immune cell adoptive transfer from immunized mice using irradiated B16 cells and gp100-specific (Pmel-1) TCR transgenic mice ($P<0.05$, vs cell transfer alone). Consequently, employment of a transcriptional modulation strategy using HDACis might prove to be a useful pretreatment for human melanoma immunotherapy.

Journal of Investigative Dermatology (2008) **128,** 1506–1516; doi:10.1038/sj.jid.5701216; published online 10 January 2008

INTRODUCTION

Great efforts have been made in the field of tumor immunology, and attempts to enhance cellular immune responses have used various cancer antigens and immunizing vectors (Rosenberg, 2004; Gattinoni *et al.*, 2006). Although these strategies allow for the generation of immune T cells that recognize antigenic peptides present on tumor cells, the regression of growing tumors in patients treated with active immunization has been sporadic and rare (Rosenberg *et al.*, 2004). In fact, a variety of factors that limit tumor regression despite the *in vivo* generation of antitumor T cells have been reported (Rosenberg and Dudley, 2004), and it is therefore necessary to overcome many tumor and lymphocyte factors that cause the tumor-escape mechanisms. Targeting key survival pathways in tumor cells, particularly those that allow cancer cells to prevent host immune attacks, is an attractive approach when aiming for an increase in the effectiveness of cancer immunotherapy.

There are emerging data suggesting that aberrant transcriptional repression of genes to control cell growth and differentiation is a hallmark of malignancy (Herman and Baylin, 2003). With melanoma, as with many other cancers, alteration of histone deacetylases (HDACs) underlies the transcriptional repression (Klisovic *et al.*, 2003; Kobayashi *et al.*, 2006). Thus, blockade of HDACs might restore global gene expression in cancer cells, making them sensitive to cell cycle arrest, differentiation, and apoptotic cell death (Johnstone and Licht, 2003; Minucci and Pelicci, 2006). The action mode of histone deacetylase inhibitors (HDACis), as the transcriptional modulator, differs from that of other anticancer agents (Marks *et al.*, 2001), and HDACis are expected to be effective for many cancer types that resist conventional chemotherapy (Marks *et al.*, 2001; Minucci and Pelicci, 2006). Indeed, HDACis have shown cytotoxicity in a variety of human and rodent cancer cells *in vitro* and *in vivo* (Hoshikawa *et al.*, 1994), some of which are being tested in clinical studies (Minucci and Pelicci, 2006).

Depsipeptide (also referred to as FK228 and FR901228) may be considered a promising HDACi for human melanoma. It was originally isolated from *Chromobacterium violaceum* (no. 968) as a compound that reversed the

[1]*Division of Organ Replacement Research, Center for Molecular Medicine, Jichi Medical University, Shimotuke, Tochigi, Japan;* [2]*Department of Dermatology, Jichi Medical University, Shimotuke, Tochigi, Japan;* [3]*Division of Stem Cell Regulation, Center for Molecular Medicine, Jichi Medical University, Shimotuke, Tochigi, Japan and* [4]*Division of Medical Oncology, Tochigi Cancer Center, Utsunomiya, Tochigi, Japan*

Correspondence: Dr Takashi Murakami, Division of Organ Replacement Research, Center for Molecular Medicine, Jichi Medical University, 3311-1 Yakushiji, Shimotsuke, Tochigi 329-0498, Japan.
E-mail: takmu@jichi.ac.jp

Abbreviations: CTL, cytotoxic T lymphocyte; FasL, Fas ligand; FCS, fetal calf serum; HDAC, histone deacetylase; HDACi, histone deacetylase inhibitor; MHC, major histocompatibility complex; PE, phycoerythrin; RT-PCR, reverse transcription-PCR; s.c., subcutaneous

Received 7 May 2007; revised 14 September 2007; accepted 3 November 2007; published online 10 January 2008

malignant phenotype of H-ras-transformed fibroblasts by blocking the $p21^{ras}$-mediated signal transduction pathway (Ueda *et al.*, 1994a, b). Depsipeptide suppressed cell proliferation and induced apoptosis in human uveal melanoma cell lines at relatively high doses (Klisovic *et al.*, 2003) and produced substantial therapeutic effects on various malignancies (Minucci and Pelicci, 2006). In our previous study to determine the molecular basis of its cytotoxic effect, depsipeptide suppressed the Ras-mitogen-activated protein kinase signaling pathway through Rap1 upregulation, leading to apoptosis in human melanoma cells (Kobayashi *et al.*, 2006). Herein, we show that depsipeptide sensitized poorly immunogenic murine B16 melanoma cells to the Fas ligand and that a limited dose of depsipeptide suppressed *in vivo* growth of B16/F10 in combination with adoptive immune cell transfer therapy. Consequently, a transcriptional modulation strategy using HDACis might prove to be a useful adjunct in human immunotherapy strategies against cancer.

RESULTS

Depsipeptide enhances expression of gp100/pmel17 melanoma antigen in melanoma cell lines

Our recent DNA micro-array study revealed that the HDACi depsipeptide markedly enhanced mRNA expression of gp100/pmel17 melanoma antigen in MM-LH human melanoma cells (15-fold increase) (Kobayashi *et al.*, 2006). Thus, we initially hypothesized that gp100/pmel17 would be a potential target of depsipeptide in human melanoma cells. The expression of gp100/pmel17 in human melanoma cell lines was examined by reverse transcription-PCR (RT-PCR) (Figure 1a). All melanoma cell lines examined showed strong enhancement of gp100/pmel17 mRNA expression after exposure to depsipeptide (10 nM) for 16 hours, whereas normal healthy melanocytes were not affected by the same dose of depsipeptide. The expression of gp100/pmel17 by depsipeptide was moderately enhanced in murine B16/F10 melanoma cells.

To characterize the effects of depsipeptide in a murine model of melanoma, we examined the ability of depsipeptide to induce histone acetylation in B16/F10 cells (Figure 1b). Basal acetylation of histone H3 (lysine residue 9) was detected, and subsequent experiments revealed that the acetylation level of histone H3 (lysine residues 9 and 18) increased significantly after a 24 hour exposure to 1–10 nM depsipeptide. Furthermore, major histocompatibility complex (MHC) class I ($H2\text{-}D^b$) and Fas (CD95) death receptor expression were enhanced in B16/F10 cells exposed to depsipeptide (Figure 1c). In human melanoma cell lines, to depsipeptide resulted in moderately enhanced MHC class I expression but not Fas expression (Figure S1). Thus, a 1–10 nM depsipeptide dose could sufficiently modulate murine B16/F10 melanoma cells within 16 hours *in vitro*, suggesting that a limited dose of depsipeptide may be effective for recognition and sensitization of immune cell-mediated tumor destruction in mice.

A limited dose of depsipeptide moderately induces apoptosis and cell cycle arrest in murine B16 melanoma cells

We have shown previously that depsipeptide induces apoptotic cell death in human melanoma cell lines (Kobayashi

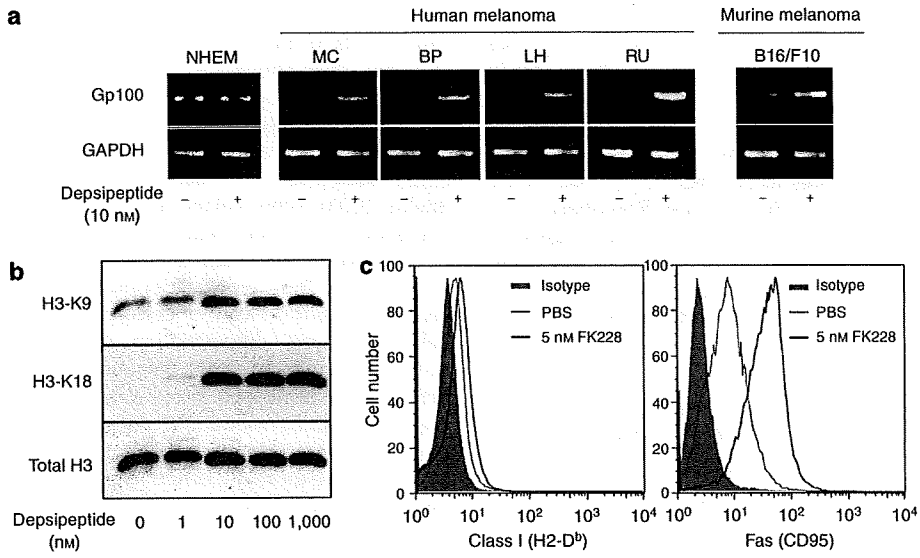

Figure 1. Depsipeptide enhances expression of gp100/pmel17 melanoma antigen. (**a**) RT-PCR analysis of gp100/pmel17 transcript. Total RNA was extracted from each melanoma cell line after exposure to depsipeptide (10 nM) for 16 hours. PCR was performed with primers as described in Materials and Methods. GAPDH, glyceraldehyde-3-phosphate dehydrogenase (as an internal control); NHEM, normal healthy melanocytes; MC (RPM-MC), BP (MM-BP), LH (MM-LH), and RU (MM-RU) are human melanoma cell lines. One of three independent experiments with similar results is shown. (**b**) Effect of depsipeptide on histone deacetylation in B16/F10 cells. B16/F10 cells (2×10^6) were exposed to depsipeptide at the indicated concentration for 16 hours. Cells were lysed and analyzed for anti-acetyl-histone H3 (Lys 9), anti-acetyl-histone H3 (Lys 18) and anti-histone H3 by western blotting. (**c**) Expression of MHC class I ($H\text{-}2D^b$) and Fas (CD95) in B16/F10 cells following exposure to depsipeptide. B16/F10 cells were exposed to depsipeptide at the indicated concentration for 16 hours and stained with PE-conjugated anti-$H\text{-}2D^b$ or Fas mAb. The control was treated with PBS. One of 2–3 independent experiments with similar results is shown.

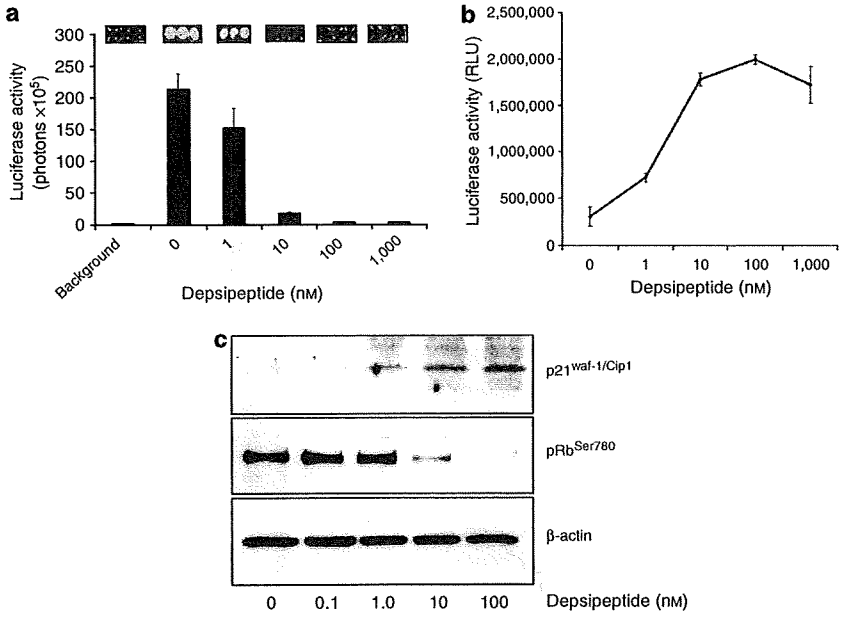

Figure 2. Depsipeptide activates caspase-3/7 and accompanies cell cycle arrest in B16/F10 cells. (**a**) Luc-B16/F10 cells (1×10^5) were plated onto 48-well plates at the indicated number and exposed to depsipeptide at the indicated concentration for 16 hours. Luciferase activity (photon counts) was then evaluated in the presence of D-luciferin. (**b**) Caspase-3/7 activity was quantified for 16 hours following treatment at the indicated concentration of depsipeptide in B16/F10 cells (2×10^4). The Caspase-Glo 3/7 Assay system (Promega) was used according to the manufacturer's instructions. The background luminescence associated with the cell culture and assay reagent (blank reaction) was subtracted from experimental values. (**c**) Western blot analysis of $p21^{Waf1/Cip1}$ and phospho-RB (Ser780) 16 hours following treatment at the indicated concentration of depsipeptide. β-actin was used as an internal control. One of two independent experiments with similar results is shown.

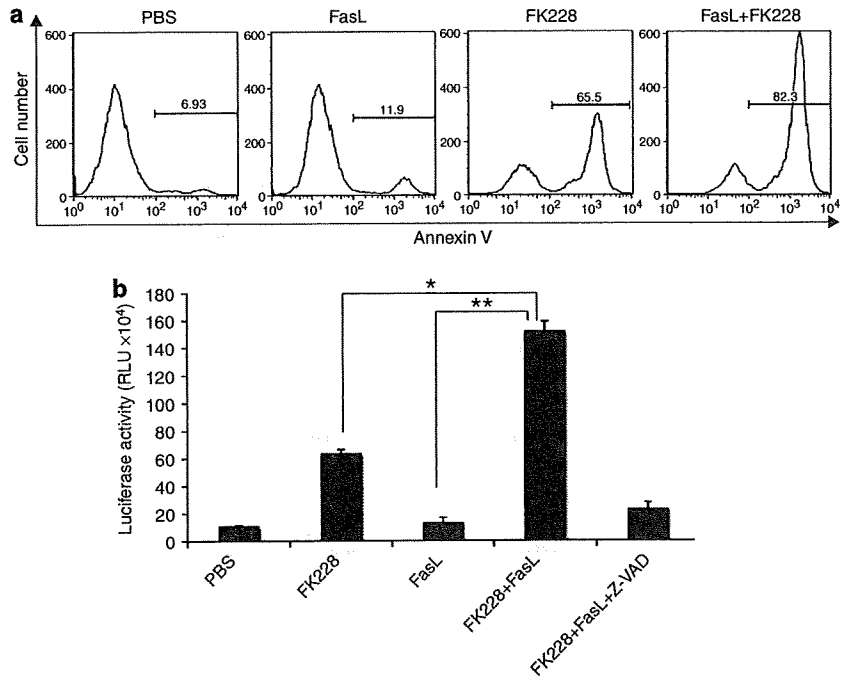

Figure 3. A sublethal dose of depsipeptide with Fas engagement synergistically promotes apoptotic cell death in B16/F10 cells *in vitro*. (**a**) B16/F10 cells (1×10^6) were treated with depsipeptide (5 nM) and recombinant FLAG-tagged FasL (10 ng ml^{-1}) and multimerized with anti-FLAG M2 antibodies (1 mg ml^{-1}) for 16 hours. Cells were then collected and stained with annexin-V-FITC. One of two independent experiments with similar results is shown. (**b**) Caspase-3/7 activity after exposure to depsipeptide with Fas engagement. The Caspase-Glo 3/7 Assay system (Promega) was used as described above. $*P<0.05$; $**P<0.001$ (Student's *t*-test).

et al., 2006). As photon emission from luciferase-expressing luc-B16/F10 cells was highly correlated with viable cell number (Sato *et al.*, 2006), we examined a sublethal dose of depsipeptide on murine B16/F10 melanoma cells (Figure 2a). Results revealed that depsipeptide decreased tumor-derived photons in a dose-dependent manner. Furthermore, caspase-3/7 activity in unmanipulated B16/F10 cells also increased linearly after a 24 hour exposure to 1–10 nM depsipeptide (Figure 2b), with the median dose of depsipeptide (ED_{50}) being 5.34 nM. The increase in caspase-3/7 activity was accompanied by a dose-dependent increase in the expression of the cell cycle regulator $p21^{Waf/Cip1}$, and the Rb protein was dephosphorylated at the critical residue Ser^{780} for the cell cycle (Figure 2c). Thus, a sublethal dose of depsipeptide could moderately induce apoptosis and cell cycle arrest in murine B16/F10 melanoma cells.

Depsipeptide with Fas death receptor engagement synergistically promotes apoptosis in B16/F10 melanoma cells

In mechanisms associated with lymphocyte-mediated tumor killing, the Fas and Fas ligand (FasL) system is a well-known major pathway in mice (Kagi *et al.*, 1994; Caldwell *et al.*, 2003; Lee *et al.*, 2006). We therefore examined whether a sublethal dose of depsipeptide (ED_{50}: 5 nM) promoted FasL-triggered apoptosis. B16/F10 cells were exposed to depsipeptide in the presence or absence of multimerized FasL, which was measured by annexin-V staining (Figure 3a). In the presence of depsipeptide, B16/F10 cells readily induced apoptotic cell death after Fas–FasL crosslinking, whereas B16/F10 cells were resistant to apoptosis with Fas crosslinking alone. Caspase-3/7 activity was also synergistically enhanced in the presence of depsipeptide and FasL (Figure 3b). Pan-caspase inhibition in tumor cells treated with Z-VAD-fmk almost totally cancelled the enhanced cytotoxic effect.

We next investigated whether a sublethal dose of depsipeptide promoted cytotoxicity induced by melanoma antigen-specific cytotoxic T lymphocytes (CTLs). To generate B16/F10-specific CTLs, C57BL/6 mice were immunized twice by subcutaneous (s.c.) injection of irradiated IL-12/IL-18-transduced B16/F10 cells (Sato *et al.*, 2006). Spleen cells from immunized mice showed enhanced production of IFN-γ (Figure 4a) and moderate killing activity with respect to B16/F10 cells (data not shown). Strikingly, the spleen cells demonstrated efficient killing of luc-B16/F10 cells in the presence of depsipeptide (Figure 4b). Furthermore, we investigated whether depsipeptide-exposed luc-B16/F10 cells could be killed by $CD8^+$ T cells from a transgenic mouse (Pmel-1), which expressed Vα2Vβ13 TCR from H-$2D^b$-restricted murine gp100-specific clone no. 9 T cells (Overwijk *et al.*, 2003). As shown in Figure 5a, Pmel-1 T cells were also capable of efficiently killing depsipeptide-exposed luc-B16/F10 cells. Depsipeptide at 5 nM moderately enhanced the surface expression of FasL in antigen-activated Pmel-1 T cells (Figure 5b). Furthermore, to examine whether pmel-1 CTL killing of luc-B16/F10 was primarily mediated by Fas–FasL-dependent pathway, we assessed the effect of anti-FasL neutralizing antibodies on the luc-B16/F10 killing. Anti-FasL mAb (20 μg ml^{-1}) inhibited Pmel-mediated killing of

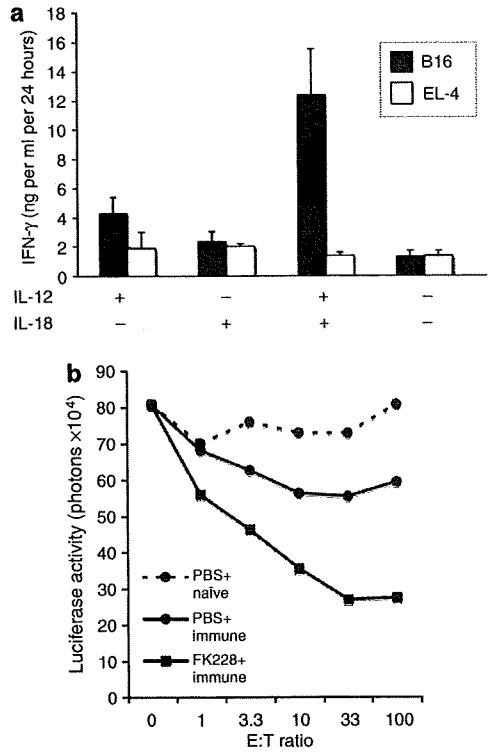

Figure 4. Melanoma-specific CTLs with depsipeptide can synergistically kill B16/F10 cells *in vitro*. (**a**) IFN-γ levels from splenocytes were assayed by ELISA. Splenocytes (2×10^5) were isolated after the second immunization using irradiated IL-12/IL-18 cDNA-transduced B16/F10 cells and were co-cultured for 24 hours with 1×10^5 target cells (irradiated with 80 Gy). The IFN-γ concentration of the supernatants was measured using a mouse IFN-γ immunoassay kit (R&D Systems, Minneapolis, MN) according to the manufacturer's instructions. EL-4 thymoma cells were used for control H-2^b tumor cells for a B16-specific IFN-γ increase. Error bar, SD ($n=3$). A representative result of three independent experiments with similar results is shown. (**b**) Cytotoxic assay against depsipeptide-exposed luc-B16/F10 cells. C57BL/6 mice were immunized by s.c. injection of irradiated IL-12/IL-18 cDNA-transduced B16/F10 cells. Spleen cells were isolated and used as effectors at the indicated effector-to-target (E:T) ratios. Photons represent cell viability from luc-B16/F10 cells 10 hours following incubation with effector lymphocytes. Data are shown as the average of triplicate assays.

depsipeptide-treated luc-B16/F10 cells at lower effector-to-target ratios (Figure 5c). This anti-FasL mAb could not sufficiently block the Pmel-mediated killing even at a high concentration (50 μg ml^{-1}, Figure 5d). Thus, in regard to the mechanism underlying the synergistic effect of depsipeptide and CTL cells, the CTL-mediated killing of B16 cells was not completely dependent on Fas–FasL interactions.

Depsipeptide increases perforin in activated $CD8^+$ T lymphocytes

We further addressed the effects of depsipeptide on activated $CD8^+$ T cells *in vitro*. The trypan blue exclusion test showed that depsipeptide at 5 nM had little effect on viability of antigen-activated Pmel-1 CTLs within 24 hours (data not shown). An alternative hypothesis is that depsipeptide may enhance immune effector cell function to produce the

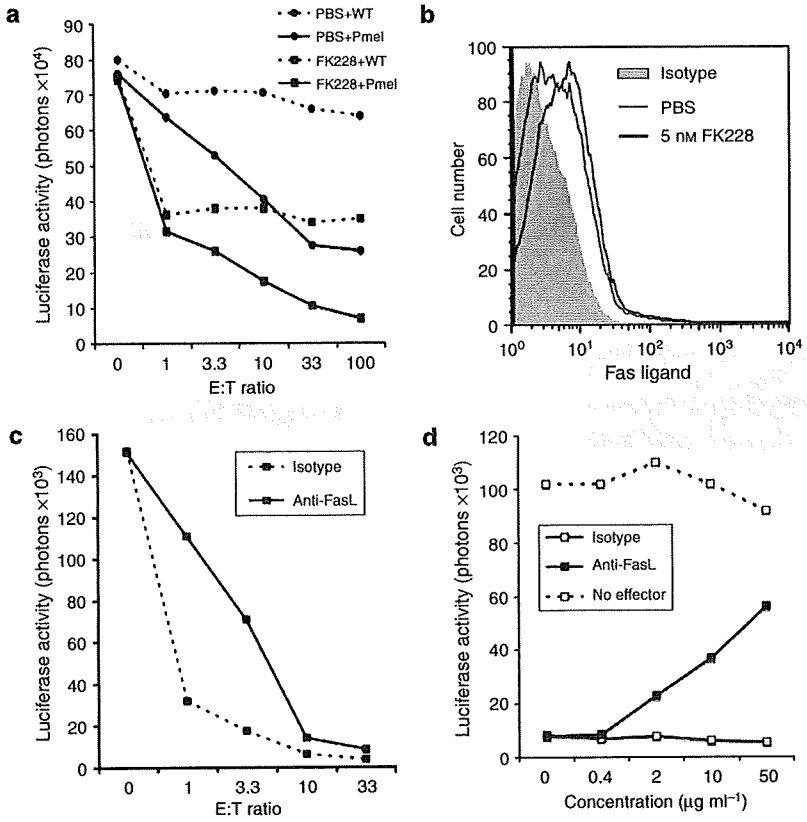

Figure 5. Gp100-specific CTLs with depsipeptide can synergistically kill B16/F10 cells *in vitro*. (**a**) Killing of depsipeptide-exposed luc-B16/F10 cells by gp100-specific CD8$^+$ T cells from a transgenic mouse (Pmel-1). Pmel-1 cells were used as effectors at the indicated effector-to-target (E:T) ratios. One of three independent experiments with similar results is shown. (**b**) Expression of FasL (CD178) in Pmel-1 T cells following exposure to depsipeptide. Antigen-stimulated Pmel-1 T cells were exposed to depsipeptide at 5 nM for 16 hours and stained with PE-conjugated anti-FasL mAb. (**c**) Effect of neutralizing anti-FasL mAb on Pmel-1 CTL-mediated B16/F10 killing. Depsipeptide (5 nM)-exposed luc-B16/F10 cells were co-incubated with Pmel-1 CTLs for 16 hours in the presence of ant-FasL mAb (20 μg ml^{-1}) or isotype-matched control Ab (20 μg ml^{-1}). (**d**) Depsipeptide (5 nM)-exposed luc-B16/F10 cells were incubated with Pmel-1 CTLs at a 10:1 (E:T) ratio for 16 hours with various concentrations of ant-FasL mAb. One of two independent experiments with similar results is shown.

antitumor response. Pmel-1 T cells were exposed to depsipeptide in the presence or absence of antigen stimulation, and expression of perforin was analyzed using flow cytometry (Figure 6a). Although perforin expression levels did not alter in unstimulated Pmel-1 T cells following exposure to 5 nM depsipeptide for 24 hours, cells that express perforin increased in antigen-stimulated Pmel-1 T cells. To address whether perforin mRNA expression in Pmel-1 T cells could be altered by exposure to depsipeptide, RT-PCR analysis was performed (Figure 6b). The results demonstrated that levels of perforin mRNA did not alter following exposure to multiple concentrations of depsipeptide. These results, therefore, suggest that perforin expression by exposure to depsipeptide is regulated at post-transcriptional levels. An increase of perforin was also observed in healthy human peripheral CD8$^+$ T cells stimulated with phytohemagglutinin-P (PHA-P) for 24 hours (Figure 6c) and an accumulation of perforin was observed in a small number of these T cells (Figure S2). These results suggest that depsipeptide potentially increases the number of cells that express perforin in murine-activated CD8$^+$ T cells and that it enhances intracellular perforin accumulation in human T cells. These results may support the notion of an antitumor response in the host.

Inhibition of tumor growth of B16/F10 by a combination of depsipeptide with immune cell adoptive transfer therapy

To examine whether a sublethal dose of depsipeptide sensitizes B16/F10 cells *in vivo* for adoptive immunotherapy, growth retardation of established B16/F10 s.c. tumor in C57BL/6 mice (see Materials and Methods) was monitored after intraperitoneal injection of depsipeptide and subsequent adoptive transfer of Pmel-1 CTLs (Figure 7a). Depsipeptide intraperitoneal administration was performed for 3 days at the indicated doses. Established B16/F10 s.c. tumor growth was retarded with 2 mg kg^{-1} of depsipeptide at 7 days post-Pmel-1 CTL transfer. The acetylation level of histone H3 (lysine 18) also increased following depsipeptide treatment at target tumor sites (Figure 7b). Notably, this modulation was preferentially observed in the margin and perivascular area of the formed tumor (Figure S3a). A moderate induction

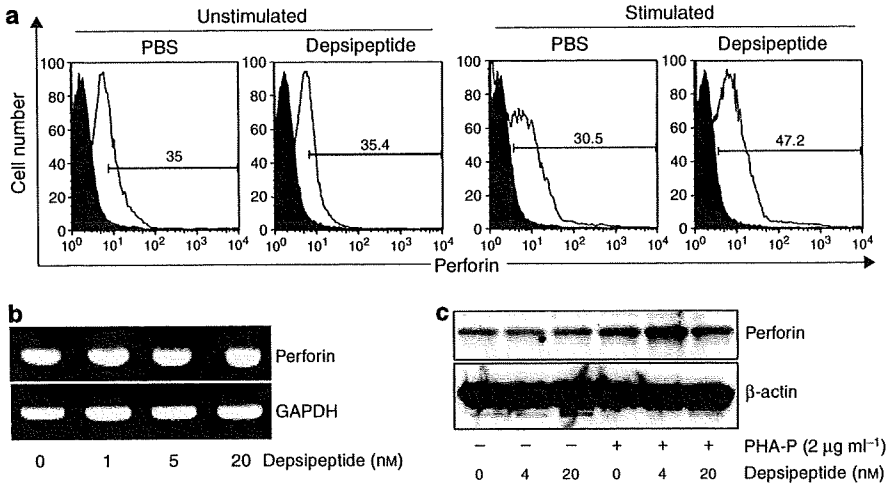

Figure 6. Effect of depsipeptide on perforin expression in effector T cells. (**a**) Increase of perforin-expressing antigen-stimulated pmel-1 T cells by exposure to depsipeptide (5 nM). Primary or antigen-stimulated Pmel-1 T cells (Thy1.1$^+$) with or without depsipeptide (5 nM) for 16 hours were stained by FITC-conjugated anti-mouse perforin mAb after treatment with a Fixation & Permeabilization Kit (eBioscience). Shaded area represents isotype-matched control staining. (**b**) Antigen-stimulated Pmel-1 T cells were treated with depsipeptide at various concentrations for 16 hours, and then perforin mRNA was analyzed by RT-PCR (glyceraldehyde-3-phosphate dehydrogenase (GAPDH), an internal control). (**c**) Human CD8$^+$ T cells were purified from peripheral blood mononuclear cells of healthy volunteers by magnetic bead selection and stimulated with or without PHA-P (2 μg ml^{-1}) *in vitro* for 24 hours. Cells were then lysed and probed for perforin and actin (as an internal control) by western blotting.

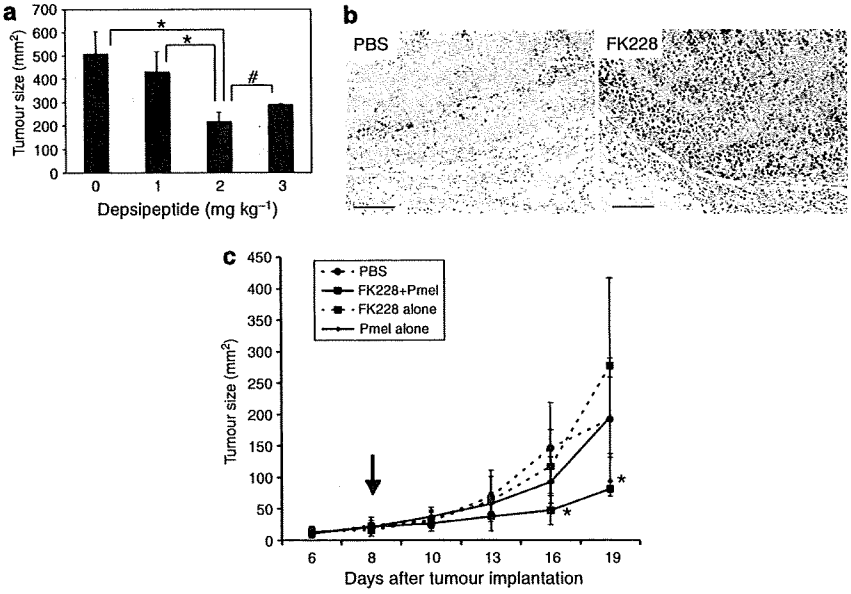

Figure 7. A limited dose of depsipeptide enhances CTL-mediated Luc-B16/F10 cell killing *in vivo*. (**a**) Effect of depsipeptide on B16/F10 tumor growth *in vivo*. B16/F10 cells (1×10^6) were inoculated subcutaneously into the abdominal skin of mice (day 0). A visible tumor in each mouse was established at day 7 after tumor implantation (average size: $122 \pm 20\,mm^2$), and mice were randomized and divided into four groups before treatment. Depsipeptide was administered intraperitoneally into mice from days 7–9 (only for 3 days) at the indicated dose, and activated Pmel-T cells (4×10^6) were subsequently injected intravenously into the tail vein of mice. Tumor growth was measured at day 21 after tumor implantation. The error bars represent the mean ± SD ($n = 4$). *$P < 0.05$; $^{\#}P > 0.3$ (Mann–Whitney *U*-test). (**b**) Effect of depsipeptide on histone deacetylation in a subcutaneous tumor of B16/F10 cells. Established B16/F10 skin tumors 1 day after the final depsipeptide administration (2 mg kg^{-1}) were probed for acetyl-histone H3 (Lys 18) by immunohistochemistry (Bar = 100 μm). (**c**) Depsipeptide enhances CTL-mediated B16/F10 tumor killing *in vivo*. B16/F10 cells (5×10^5) were inoculated subcutaneously into the abdominal skin of mice (day 0). A visible tumor in each mouse was established at day 5 after tumor implantation. Depsipeptide (2 mg kg^{-1}) was administered intraperitoneally into mice from days 6–8 (for 3 days), and Pmel-1 CTLs (4×10^6) were subsequently injected intravenously into the tail vein of mice (indicated by the arrow). Tumor growth was monitored every 2–3 days after tumor implantation. The error bars represent the mean ± SD ($n = 5$–6). *$P < 0.05$ (Kruskal–Wallis test; at days 16 and 19 after tumor implantation). One of three independent experiments with similar results is shown.

of gp100/pmel17 was also observed by RT-PCR assay (Figure S3b). Thus, these data demonstrate that a limited dose of depsipeptide ($2\,mg\,kg^{-1}$) sufficiently sensitized B16/F10 cells *in vivo* for adoptive immunotherapy. Regarding the perforin modulation, we could not determine whether perforin induction occurred *in vivo* by FACS analysis.

We further investigated whether s.c. tumor growth of B16/F10 cells could be inhibited by the adoptive transfer of Pmel-1 CTLs in combination with depsipeptide (Figure 7c). After waiting about a week for tumor growth, $2\,mg\,kg^{-1}$ of depsipeptide was administered via the intra-peritoneal route, followed by the adoptive transfer of Pmel-1 CTLs. In contrast to either CTL transfer alone or depsipeptide pretreatment alone, this combinatorial treatment strikingly suppressed B16/F10 tumor growth. Moreover, we examined whether the above depsipeptide pretreatment and a similar CTL transfer could suppress metastatic tumor growth (Figure 8). Luc-B16/F10 cells were intravenously injected into the tail vain of C57BL/6 mice, and pulmonary metastasis of luc-B16/F10 cells was monitored through luciferase-based luminescent imaging. After waiting about a week for tumor growth, animals were treated with $2\,mg\,kg^{-1}$ of depsipeptide for 3 days, followed by the adoptive transfer of CTLs, which were generated by immunization using irradiated IL-12/IL-18-transduced B16/F10 cells. This combinatorial treatment significantly suppressed tumor-derived photons in pulmonary metastases 21 days following tumor injection. Similar suppression of pulmonary metastases was obtained by adoptive transfer of Pmel-1-derived CTLs (data not shown). Thus, these results demonstrate that sensitization using a limited dose of depsipeptide increases the efficacy of adoptive immunotherapy for established tumors.

DISCUSSION

Cellular unresponsiveness of solid tumor through aberrant transcriptional regulation represents a critical barrier that limits the therapeutic potential of adoptively transferred autologous CTLs in patients with cancer. Herein, we have demonstrated that tumor sensitization with depsipeptide is effective for adoptive immunotherapy against murine B16/F10 melanoma. The remarkable features presented in this study include the following: (1) depsipeptide upregulated gp100/pmel17 melanoma antigen; (2) a limited dose of depsipeptide was able to sufficiently sensitize B16/F10 cells for Fas-mediated apoptosis; (3) depsipeptide increased the perforin-expressing CTLs in post-transcriptional levels; and (4) adoptive cell transfer in combination with depsipeptide led to effective tumor growth suppression.

Emerging evidence suggests that there are a variety of factors that limit tumor regression in the host–tumor interaction. For example, cancer progression often takes place despite the presence of circulating cancer-specific CTLs. Even with patients in whom large numbers of highly activated tumor-specific CTLs have been infused, clinical improvement has been difficult to achieve (Dudley *et al.*, 2001; Rosenberg, 2004). For example, recent evidence concerning host factors suggests that regulatory elements of the immune responses, including $CD4^+CD25^+$ regulatory T cells (Tregs), inhibit the ability of CTLs to produce effective antitumor responses (Antony and Restifo, 2005; Dannull *et al.*, 2005). In regard to tumor-escape factors, many aggressive tumors do not express the tumor antigen or MHC (HLA) antigen (Ferrone and Marincola, 1995; Cabrera *et al.*, 2003). Moreover, many cancer types lack sufficient apoptotic cell death pathways through the aberrant transcription (Johnstone *et al.*, 2002; Maecker *et al.*, 2002). It is theoretically essential to overcome these tumor-escape factors for efficient cancer immunotherapy, and perhaps to manipulate the tumor, as well as the host, before adoptive immune cell transfer.

HDACs are considered among the most promising targets in drug development for cancer, and some HDACi, including depsipeptide (FK228), are currently being tested in phase I and II clinical trials (Minucci and Pelicci, 2006). HDACi is capable of inducing varying degrees of growth arrest,

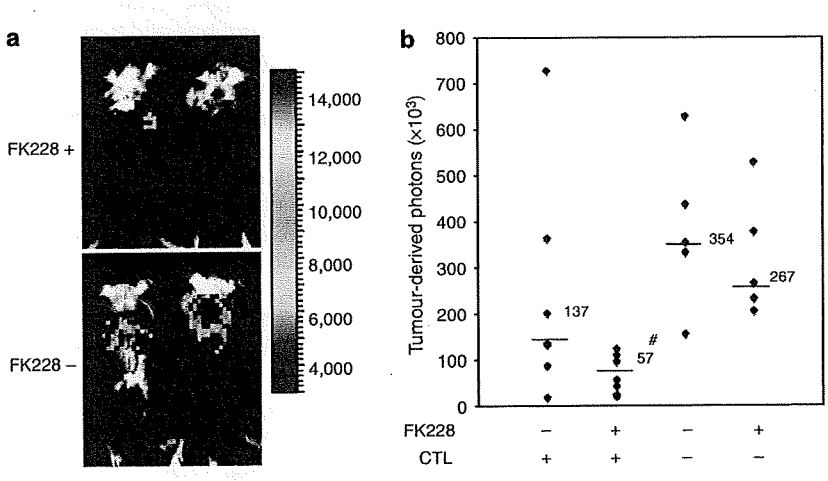

Figure 8. Depsipeptide pretreatment and B16-specific CTLs transfer suppress metastatic tumor growth of B16/F10 cells. (**a**) Representative luciferase images of luc-B16/F10 metastatic lung tumor at day 15 after combinatorial therapy of depsipeptide ($2\,mg\,kg^{-1}$) and immune cell adoptive transfer from immunized mice using irradiated IL-12/IL-18-transduced B16/F10 cells. (**b**) Photon counting of luc-B16/F10-pulmonary metastasis at day 21 ($n=6$–7). $^{\#}P<0.01$ (Kruskal–Wallis test). One of three independent experiments with similar results is shown.

differentiation, or apoptosis of cancer cells (Johnstone *et al.*, 2002; Minucci and Pelicci, 2006). In addition, normal fibroblasts and melanocytes are almost always considerably more resistant than tumor cells to depsipeptide (Kobayashi *et al.*, 2006; Minucci and Pelicci, 2006), suggesting this effect may be specific to malignant cells. We demonstrated the potential upregulation of MHC class I molecules by depsipeptide treatment. As the MHC class I molecule is released from the endoplasmic reticulum only after the peptide has bound and is allowed to reach the cell surface (Williams *et al.*, 2002), this upregulation could provide substantial benefits for the immunological recognition. However, there are abnormalities in the expression and/or function of various components of the MHC class I antigen-processing pathway in human malignant cells (Seliger *et al.*, 2000; Chang and Ferrone, 2007), and it remains to be elucidated whether HDACi affects various components of the protein-processing machinery.

Although the clinical use of depsipeptide when administered alone showed partial and complete responses in patients with hematological malignancy (Piekarz *et al.* 2001, 2004; Byrd *et al.*, 2005), only a partially objective response was observed in solid cancer patients (Sandor *et al.*, 2002; Stadler *et al.*, 2006), suggesting that depsipeptide alone appears far from beneficial in the treatment of cancer patients. However, moving the focus onto the modulation of tumor factors and targeting HDACs could provide great benefits, particularly for selective immunotherapy against cancer. Intriguingly, HDACi could activate components of death receptor pathways, including FasL and tumor necrosis factor-related apoptosis-inducing ligand (TRAIL) (Nakata *et al.*, 2004; Singh *et al.*, 2005; Earel *et al.*, 2006). In fact, B16/F10 cells are less immunogenic and highly resistant to a variety of apoptotic stimuli if they are not manipulated (Avent *et al.*, 1979; Tsai *et al.*, 1997; Kalechman *et al.*, 1998). Nonetheless, exposure of B16 cells to a limited dose of depsipeptide induced cell surface expression of Fas and MHC class I, and the enforced Fas-engagement synergistically increased caspase-3/7 activity of B16/F10 cells in the presence of depsipeptide (Figure 3). Furthermore, these changes successfully provided CTLs with an enhanced ability to recognize and destroy target tumor cells (Figures 4 and 5).

Indeed, it has been demonstrated that HDACi synergizes with exogenously added TRAIL to induce apoptosis of various human solid tumor cell lines *in vitro* (Inoue *et al.*, 2004; Nakata *et al.*, 2004; Singh *et al.*, 2005; Lundqvist *et al.*, 2006). While the TRAIL system seems to be relatively major in the effect of HDACi on the human death receptor pathway, it has been suggested that the effect of HDACi on the death receptor pathway may not be universal (Minucci and Pelicci, 2006). We could not obtain a synergistic effect of depsipeptide with FasL in Fas-negative human MM-LH cells, and mouse Pmel-1 T cells did not express TRAIL on the cell surface (unpublished data). The Fas–FasL system is well known as the major pathway of CTL-mediated tumor destruction in murine models (Kagi *et al.*, 1994; Caldwell *et al.*, 2003; Lee *et al.*, 2006), and therefore some differences between species should be considered for the major death receptor pathway. However, current animal studies have demonstrated that the augmented tumoricidal effects of tumor-specific CTLs induced as a consequence of depsipeptide sensitization resulted in melanoma cells that produced CTL-mediated cytotoxicity *in vivo*. A limited administration of depsipeptide also sufficiently modulated the acetylation level of histone H3 at the tumor site (Figure 7b). These findings may provide the rationale for protocols that pretreat cancer patients with depsipeptide to potentiate adoptive immune therapy.

Emerging experimental data indicate that lymphodepletion using cyclophosphamide before adoptive transfer of tumor-specific T lymphocytes plays a key role in enhancing treatment efficacy by eliminating regulatory T cells and competing elements of the immune system (Ghiringhelli *et al.*, 2004; Lutsiak *et al.*, 2005). Furthermore, pretreatment with cyclophosphamide contributes to the elimination of immunosuppressive cells such as $CD4^+CD25^+$ Treg in patients with cancer and the depletion of endogenous cells that compete for the activation of cytokines (known as the "cytokine sink") to maximize the exposure of homeostatic cytokines to the transferred CTLs (Gattinoni *et al.*, 2006). In addition to this pretreatment, depsipeptide may safely be added to reduce barrier tumor factors limiting the therapeutic potential of adoptively transferred CTLs. We further demonstrated that depsipeptide increased the level of perforin in activated T cells to varying degrees: the number of perforin-expressing CTLs increased in mice, whereas an accumulation of perforin was observed in humans. Perforin release by T cells in conjunction with granzymes induces an apoptotic cascade in target cells (Kagi *et al.*, 1994). In fact, Palmer *et al.* (2004) showed that there was a B16 cell-dependent release of perforin after adoptive cell transfer of pmel-1 T cells, in which caspase-3 activation was also shown at the tumor site as a consequence of the downstream activation of perforin. Therefore, the residual depsipeptide in the plasma of pretreated hosts could be expected to release large amounts of toxic granules to the target tumor at the sites and, in combination with cyclophosphamide, the use of depsipeptide may be considered for host and tumor modulation before adoptive tumor-specific CTL transfer.

The therapeutic options for patients with metastatic disease remain limited, and the majority of these patients will develop a local or systemic recurrence. A variety of human cancers such as melanoma and breast, colon, and prostate cancers aberrantly express the chemokine receptor CXCR4 (Balkwill, 2004; Kakinuma and Hwang, 2006; Zlotnik, 2006), and its activation through prosurvival pathways such as Akt has been implicated as a mechanism by which cancer cells evade host immunity (Murakami *et al.*, 2003) and increase their metastatic properties (Kakinuma and Hwang, 2006). Recently, Lee *et al.* (2006) reported that sensitization of B16 cells with a CXCR4 antagonistic peptide increases the efficacy of immunotherapy for pulmonary metastases, suggesting that the inhibition of tumor factor is an effective strategy for melanoma immunotherapy. Herein, we also provide compelling *in vitro* and *in vivo* data suggesting that sensitization of less immunogenic B16 cells with depsipeptide facilitates the efficacy of immunotherapy

for established pulmonary metastases. Further investigations based on the findings of this study, especially those incorporating *in vivo* techniques, should improve the design of optimized clinical protocols.

MATERIALS AND METHODS

Animals, cells, and reagents

Male C57BL/6 J mice (8–12 weeks old) were purchased from Charles River Japan Inc. (Tsukuba, Japan). Pmel-1 TCR pmel-1 +/Thy1.1 + transgenic mice (Overwijk *et al.*, 2003) were obtained from The Jackson Laboratory (Bar Harbor, ME). All experiments in this study were approved by the animal ethics review board of Jichi Medical University and performed in accordance with the Jichi Medical University Guide for Laboratory Animals, following the principles of laboratory animal care formulated by the National Society for Medical Research.

Human melanoma cell lines RPM-MC, MM-LH, MM-BP, and MM-RU were kindly provided by Dr H. Randolph Byers (Boston University Medical School) and maintained in minimal essential medium supplemented with 10% heat-inactivated fetal calf serum (FCS) (Byers *et al.*, 1991). Murine B16/F10 melanoma cells (Fidler, 1973) and EL-4 thymoma cells (Ralph, 1973) were grown in DMEM (GIBCO, Gaithersburg, MD) with 10% FCS and supplements (Sato *et al.*, 2006). Luciferase-expressing B16/F10 (luc-B16/F10) cells were generated previously (Sato *et al.*, 2006) and maintained in DMEM with 10% FCS and supplements, including puromycin (10 $\mu g\,ml^{-1}$; Sigma-Aldrich, St Louis, MO). Normal human epidermal melanocytes were purchased from Kurabo Biomedicals (Osaka, Japan) and maintained in Medium 154S with supplement (Kobayashi *et al.*, 2006). The cultures were kept in a humidified atmosphere containing 5% CO_2 and 95% air at 37°C.

Anti-acetyl-histone H3 (Lys 9), anti-acetyl-histone H3 (Lys 18), anti-histone H3, and anti-phospho-Rb (Ser 780) antibodies were purchased from Cell Signaling Technology (Beverly, MA). Anti-mouse $p21^{Waf1/Cip1}$ (BD Pharmingen, San Diego, CA), anti-human perforin (clone δG9; BD Pharmingen), and anti-actin (sc-1616, Santa Cruz Biotechnology Inc., Santa Cruz, CA) antibodies were used for western blotting. Flow cytometric analysis involved the use of phycoerythrin (PE)-conjugated anti-mouse H-$2D^b$ mAb, PE-conjugated anti-mouse Fas (CD95) mAb, PE-conjugated anti-mouse FasL (CD178) mAb, and isotype-matched IgG controls, all of which were purchased from BD Pharmingen. FITC-conjugated anti-mouse perforin mAb (clone: eBioOMAK-D) was purchased from eBioscience (San Diego, CA). Anti-mouse FasL mAb (clone MFL3; BD Pharmingen) was used for the FasL neutralization.

The expression plasmids for mouse IL-12 and IL-18, pCAGGS-IL-12 and pcDNA-mproIL-18-mICE respectively, have been described previously (Ajiki *et al.*, 2003). Depsipeptide (FK228) was obtained from Gloucester Pharmaceuticals (Cambridge, MA).

Reverse transcription-PCR

Total RNA was extracted from cells using Isogen (Nippon Gene, Toyama, Japan). Two micrograms of total RNA was used for first-strand synthesis using SuperScript III reverse transcriptase (Invitrogen, Carlsbad, CA). PCR was then performed using ExTaq polymerase (Takara, Ohtsu, Japan). The following primers were used for gp100/pmel-17 and perforin expression analysis: human gp100/pmel-17 sense, 5′-CCTCCTTCTCTATTGCCTTG-3′; human gp100/pmel-17 anti-sense, 5′-TGTAGGAGAGGTGAGCTTCA-3′; mouse gp100 sense, 5′-GGCCAACAACACCATCATCA-3′; mouse gp100 anti-sense, 5′-GGGCAAAGATGAGAGGATGA-3′; mouse perforin sense, 5′-ACAATAACAATCCCCGGTGG-3′; mouse perforin anti-sense, 5′-TGGGATTAAAGGCGTGTGCT-3′; glyceraldehyde-3-phosphate dehydrogenase sense, 5′-GTATCGTGGAAGGACTCATG-3′; and glyceraldehyde-3-phosphate dehydrogenase anti-sense, 5′-AGT GGGTGTCGCGCTGTTGAAG-3′. PCR conditions for each set of primers included an initial treatment at 95°C for 2 minutes, followed by 30 cycles consisting of denaturation at 95°C for 15 seconds, annealing at 57°C for 30 seconds, and then extension at 72°C for 2 minutes. PCR products were analyzed using a 1% agarose gel.

Transfection and ELISA

B16/F10 cells (1×10^6) were transfected with pCAGGS-IL-12 (5 μg) and pcDNA-mproIL-18-mICE (5 μg) using Lipofectamine 2000 (Invitrogen). Immunization experiments involved irradiating IL-12/IL-18-transfected B16 cells with 80 Gy 36 hours after transfection. Irradiated cells ($1–2 \times 10^5$) were then injected twice into the subcutaneous space of C57BL/6 mice during the remaining weeks.

To analyze IFN-γ production, splenocytes ($1–2 \times 10^5$) that were isolated from immunized mice were co-cultured for 24 hours with 1×10^5 irradiated target cells, and the IFN-γ concentration of supernatants was then measured using a mouse IFN-γ immunoassay kit. All samples were assayed in triplicate.

Apoptosis and cytotoxic assay

To detect caspase-3/7 activity, B16/F10 cells (2×10^4 per well of a 96-well plate) were plated, and the Caspase-Glo 3/7 Assay system (Promega, Madison, WI) was used for analysis in accordance with the manufacturer's instructions 16 hours after the addition of depsipeptide. The background luminescence associated with the cell culture and assay reagent (blank reaction) was subtracted from experimental values. Means of triplicates were used to represent caspase-3/7 activity for the given cells. Each experiment was performed three times with similar results.

For enhancement of Fas-mediated apoptosis, B16/F10 cells were exposed to 10 $ng\,ml^{-1}$ recombinant human FLAG-tagged FasL (Apotech, San Diego, CA) in combination with 1 $mg\,ml^{-1}$ anti-FLAG M2 mAb (Sigma, St Louis, MO) for 16 hours with 5 nM depsipeptide at 37°C in the presence of 0.5% FCS, as described previously (Murakami *et al.*, 2003). After exposure of B16/F10 cells to apoptosis-enhancing conditions for 16 hours, attached (and detached) cells were collected from tissue culture plates for annexin-V staining according to the manufacturer's instructions (MEBCYTO Apoptosis Kit; MBL, Nagoya, Japan). Analysis of caspase-3/7 activity involved the assessment of 2×10^4 cells using the Caspase-Glo 3/7 Assay system (Promega).

Western blotting and flow cytometry

For western blotting, cells were lysed by sonication in radioimmuno-protein assay (RIPA) buffer (Sato *et al.*, 2006) and then centrifuged for 10 minutes at 4°C. Each cell extract (10 μg of protein) was assayed using appropriate antibodies and protein G-conjugated horseradish peroxidase (Amersham Pharmacia Biotech, Buckinghamshire, UK).

For the flow cytometric analysis, cells (1×10^6) were washed with phosphate buffered saline (PBS) and incubated with mAb for

30 minutes at 4°C. Following washing with 0.1% FCS-PBS, cells were analyzed using FACS Calibur (Becton Dickinson, Mountain View, CA) and FlowJo analysis software (Tree Star, San Carlos, CA).

Subcutaneous and intravenous tumor inoculation

Cells in an exponential growth phase were harvested by trypsinization and washed twice in PBS before injection. For the s.c. injections, cells (1×10^6) were injected into the abdominal subcutaneous space of C57BL/6 mice. Tumor growth at the skin was monitored by measurement of the two maximum perpendicular tumor diameters. For the intravenous injections to the lungs, luc-B16/F10 cells (5×10^4 in 0.2 ml PBS) were injected into the tail vein of C57BL/6 mice. Each experiment was performed 2–4 times with similar results.

In vivo bioluminescence imaging

In vivo tumor progression was examined using the noninvasive bioimaging system IVIS (Xenogen, Alameda, CA). Tumor-implanted mice were anesthetized with a mixture of ketamine and xylazine, and D-luciferin (potassium salt; Biosynth, Postfach, Switzerland) was injected into the peritoneal cavity at 2 mg per animal, which was followed immediately by the measurement of luciferase activity. The imaging system consisted of a cooled, back-thinned charge-coupled device camera to capture both a visible light photograph of the animal taken with light-emitting diodes and a luminescent image. After acquiring photographic images of each mouse, luminescent images were acquired with a 1–15 minutes exposure time (Ohsawa *et al.*, 2006; Sato *et al.*, 2006). Images were obtained with a 25 cm field of view, a binning (resolution) factor of 8, 1/f stop, and an open filter. The resulting gray scale photographic and pseudo-color luminescent images were automatically superimposed by software to facilitate the identification of any optical signal and the location on the mouse. Optical images were displayed and analyzed using Igor (WaveMetrics, Lake Oswego, OR) and IVIS Living Image (Xenogen) software packages. The signal from tumors was quantified as photons flux in units of photons per second per cm^2 per sr.

Immunohistochemistry

Removed specimens were fixed with 10% paraformaldehyde and embedded in paraffin. Tissue sections (5 μm) deparaffinized in xylene were passed through graded alcohols before being treated with 1% H_2O_2 (v/v) in H_2O for 20 minutes at room temperature. After washing the sections three times with PBS, sections were blocked for 20 minutes with 10% FCS diluted in PBS. All incubations were performed at room temperature in a moist chamber. The slides were incubated overnight at 4°C with anti-acetyl-histone H3 (Lys 18) antibody (no. 9675, Cell Signaling Technology) diluted 1:100 in blocking solution. The sections were washed in PBS and incubated with biotinylated goat anti-rabbit secondary antibody (Vector Laboratories, Burlingame, CA), and staining was visualized using a streptavidin–peroxidase conjugate (Vector Laboratories). A diaminobenzidine substrate kit (Vector Laboratories) was used for color (brown) visualization, and sections were counterstained with hematoxylin.

Statistical analysis

P-values based on two-sided Student's *t*-test, Mann–Whitney test, or Kruskal–Wallis test were obtained using the Instat software package (GraphPad, San Diego, CA). Differences between groups were considered significant if $P<0.05$.

CONFLICT OF INTEREST

The authors state no conflict of interest.

ACKNOWLEDGMENTS

We would like to thank Ms Yasuko Sakuma, Ms Yumi Ohde, and Ms Masayo Kumagai for their skillful technical assistance. This study was supported by a grant to T.M. from the Kowa Life Science Foundation (2004) and the Ministry of Education, Culture, Sports, Science and Technology (MEXT) of Japan (Project No. 17591181; 2005–2007) and by a grant from the "High-Tech Research Center" Project for Private Universities: matching fund subsidy from MEXT (2003–2007).

SUPPLEMENTARY MATERIAL

Figure S1. Expression of HLA class I (A, B, C) and Fas (CD95/Apo-1) in human melanoma cell lines following exposure to depsipeptide.

Figure S2. Increase of perforin in PHA-stimulated human T cells by exposure to depsipeptide (4 nM).

Figure S3. Effect of depsipeptide on the subcutaneous tumor of B16/F10 cells.

REFERENCES

Ajiki T, Murakami T, Kobayashi Y, Hakamata Y, Wang J, Inoue S *et al.* (2003) Long-lasting gene expression by particle-mediated intramuscular transfection modified with bupivacaine: combinatorial gene therapy with IL-12 and IL-18 cDNA against rat sarcoma at a distant site. *Cancer Gene Ther* 10:318–29

Antony PA, Restifo NP (2005) CD4+CD25+ T regulatory cells, immunotherapy of cancer, and interleukin-2. *J Immunother* 28:120–8

Avent J, Vervaert C, Seigler HF (1979) Non-specific and specific active immunotherapy in a B16 murine melanoma system. *J Surg Oncol* 12: 87–96

Balkwill F (2004) Cancer and the chemokine network. *Nat Rev Cancer* 4: 540–50

Byers HR, Etoh T, Doherty JR, Sober AJ, Mihm MC Jr (1991) Cell migration and actin organization in cultured human primary, recurrent cutaneous and metastatic melanoma. Time-lapse and image analysis. *Am J Pathol* 139:423–35

Byrd JC, Marcucci G, Parthun MR, Xiao JJ, Klisovic RB, Moran M *et al.* (2005) A phase 1 and pharmacodynamic study of depsipeptide (FK228) in chronic lymphocytic leukemia and acute myeloid leukemia. *Blood* 105:959–67

Cabrera T, Lopez-Nevot MA, Gaforio JJ, Ruiz-Cabello F, Garrido F (2003) Analysis of HLA expression in human tumor tissues. *Cancer Immunol Immunother* 52:1–9

Caldwell SA, Ryan MH, McDuffie E, Abrams SI (2003) The Fas/Fas ligand pathway is important for optimal tumor regression in a mouse model of CTL adoptive immunotherapy of experimental CMS4 lung metastases. *J Immunol* 171:2402–12

Chang CC, Ferrone S (2007) Immune selective pressure and HLA class I antigen defects in malignant lesions. *Cancer Immunol Immunother* 56: 227–36

Dannull J, Su Z, Rizzieri D, Yang BK, Coleman D, Yancey D *et al.* (2005) Enhancement of vaccine-mediated antitumor immunity in cancer patients after depletion of regulatory T cells. *J Clin Invest* 115: 3623–33

Dudley ME, Wunderlich J, Nishimura MI, Yu D, Yang JC, Topalian SL *et al.* (2001) Adoptive transfer of cloned melanoma-reactive T lymphocytes for the treatment of patients with metastatic melanoma. *J Immunother* 24:363–73

Earel JK Jr, VanOosten RL, Griffith TS (2006) Histone deacetylase inhibitors modulate the sensitivity of tumor necrosis factor-related apoptosis-inducing ligand-resistant bladder tumor cells. *Cancer Res* 66: 499–507

Ferrone S, Marincola FM (1995) Loss of HLA class I antigens by melanoma cells: molecular mechanisms, functional significance and clinical relevance. *Immunol Today* 16:487–94

Fidler IJ (1973) Selection of successive tumour lines for metastasis. *Nat New Biol* 242:148–9

Gattinoni L, Powell DJ Jr, Rosenberg SA, Restifo NP (2006) Adoptive immunotherapy for cancer: building on success. *Nat Rev Immunol* 6: 383–93

Ghiringhelli F, Larmonier N, Schmitt E, Parcellier A, Cathelin D, Garrido C *et al.* (2004) $CD4^+CD25^+$ regulatory T cells suppress tumor immunity but are sensitive to cyclophosphamide which allows immunotherapy of established tumors to be curative. *Eur J Immunol* 34:336–44

Herman JG, Baylin SB (2003) Gene silencing in cancer in association with promoter hypermethylation. *N Engl J Med* 349:2042–54

Hoshikawa Y, Kwon HJ, Yoshida M, Horinouchi S, Beppu T (1994) Trichostatin A induces morphological changes and gelsolin expression by inhibiting histone deacetylase in human carcinoma cell lines. *Exp Cell Res* 214:189–97

Inoue S, MacFarlane M, Harper N, Wheat LM, Dyer MJ, Cohen GM (2004) Histone deacetylase inhibitors potentiate TNF-related apoptosis-inducing ligand (TRAIL)-induced apoptosis in lymphoid malignancies. *Cell Death Differ* 11(Suppl 2):S193–206

Johnstone RW, Licht JD (2003) Histone deacetylase inhibitors in cancer therapy: is transcription the primary target? *Cancer Cell* 4:13–8

Johnstone RW, Ruefli AA, Lowe SW (2002) Apoptosis: a link between cancer genetics and chemotherapy. *Cell* 108:153–64

Kagi D, Vignaux F, Ledermann B, Burki K, Depraetere V, Nagata S *et al.* (1994) Fas and perforin pathways as major mechanisms of T cell-mediated cytotoxicity. *Science* 265:528–30

Kakinuma T, Hwang ST (2006) Chemokines, chemokine receptors, and cancer metastasis. *J Leukoc Biol* 79:639–51

Kalechman Y, Strassmann G, Albeck M, Sredni B (1998) Up-regulation by ammonium trichloro(dioxoethylene-0,0') tellurate (AS101) of Fas/Apo-1 expression on B16 melanoma cells: implications for the antitumor effects of AS101. *J Immunol* 161:3536–42

Klisovic DD, Katz SE, Effron D, Klisovic MI, Wickham J, Parthun MR *et al.* (2003) Depsipeptide (FR901228) inhibits proliferation and induces apoptosis in primary and metastatic human uveal melanoma cell lines. *Invest Ophthalmol Vis Sci* 44:2390–8

Kobayashi Y, Ohtsuki M, Murakami T, Kobayashi T, Sutheesophon K, Kitayama H *et al.* (2006) Histone deacetylase inhibitor FK228 suppresses the Ras-MAP kinase signaling pathway by upregulating Rap1 and induces apoptosis in malignant melanoma. *Oncogene* 25:512–24

Lee CH, Kakinuma T, Wang J, Zhang H, Palmer DC, Restifo NP *et al.* (2006) Sensitization of B16 tumor cells with a CXCR4 antagonist increases the efficacy of immunotherapy for established lung metastases. *Mol Cancer Ther* 5:2592–9

Lundqvist A, Abrams SI, Schrump DS, Alvarez G, Suffredini D, Berg M *et al.* (2006) Bortezomib and depsipeptide sensitize tumors to tumor necrosis factor-related apoptosis-inducing ligand: a novel method to potentiate natural killer cell tumor cytotoxicity. *Cancer Res* 66:7317–25

Lutsiak ME, Semnani RT, De Pascalis R, Kashmiri SV, Schlom J, Sabzevari H (2005) Inhibition of CD4(+)25(+) T regulatory cell function implicated in enhanced immune response by low-dose cyclophosphamide. *Blood* 105:2862–8

Maecker HL, Yun Z, Maecker HT, Giaccia AJ (2002) Epigenetic changes in tumor Fas levels determine immune escape and response to therapy. *Cancer Cell* 2:139–48

Marks P, Rifkind RA, Richon VM, Breslow R, Miller T, Kelly WK (2001) Histone deacetylases and cancer: causes and therapies. *Nat Rev Cancer* 1:194–202

Minucci S, Pelicci PG (2006) Histone deacetylase inhibitors and the promise of epigenetic (and more) treatments for cancer. *Nat Rev Cancer* 6:38–51

Murakami T, Cardones AR, Finkelstein SE, Restifo NP, Klaunberg BA, Nestle FO *et al.* (2003) Immune evasion by murine melanoma mediated through CC chemokine receptor-10. *J Exp Med* 198:1337–47

Nakata S, Yoshida T, Horinaka M, Shiraishi T, Wakada M, Sakai T (2004) Histone deacetylase inhibitors upregulate death receptor 5/TRAIL-R2 and sensitize apoptosis induced by TRAIL/APO2-L in human malignant tumor cells. *Oncogene* 23:6261–71

Ohsawa I, Murakami T, Uemoto S, Kobayashi E (2006) *In vivo* luminescent imaging of cyclosporin A-mediated cancer progression in rats. *Transplantation* 81:1558–67

Overwijk WW, Theoret MR, Finkelstein SE, Surman DR, de Jong LA, Vyth-Dreese FA *et al.* (2003) Tumor regression and autoimmunity after reversal of a functionally tolerant state of self-reactive CD8+ T cells. *J Exp Med* 198:569–80

Palmer DC, Balasubramaniam S, Hanada K, Wrzesinski C, Yu Z, Farid S *et al.* (2004) Vaccine-stimulated, adoptively transferred CD8+ T cells traffic indiscriminately and ubiquitously while mediating specific tumor destruction. *J Immunol* 173:7209–16

Piekarz RL, Robey R, Sandor V, Bakke S, Wilson WH, Dahmoush L *et al.* (2001) Inhibitor of histone deacetylation, depsipeptide (FR901228), in the treatment of peripheral and cutaneous T-cell lymphoma: a case report. *Blood* 98:2865–8

Piekarz RL, Robey RW, Zhan Z, Kayastha G, Sayah A, Abdeldaim AH *et al.* (2004) T-cell lymphoma as a model for the use of histone deacetylase inhibitors in cancer therapy: impact of depsipeptide on molecular markers, therapeutic targets, and mechanisms of resistance. *Blood* 103:4636–43

Ralph P (1973) Retention of lymphocyte characteristics by myelomas and theta+-lymphomas: sensitivity to cortisol and phytohemagglutinin. *J Immunol* 110:1470–5

Rosenberg SA (2004) Shedding light on immunotherapy for cancer. *N Engl J Med* 350:1461–3

Rosenberg SA, Dudley ME (2004) Cancer regression in patients with metastatic melanoma after the transfer of autologous antitumor lymphocytes. *Proc Natl Acad Sci USA* 101(Suppl 2):14639–45

Rosenberg SA, Yang JC, Restifo NP (2004) Cancer immunotherapy: moving beyond current vaccines. *Nat Med* 10:909–15

Sandor V, Bakke S, Robey RW, Kang MH, Blagosklonny MV, Bender J *et al.* (2002) Phase I trial of the histone deacetylase inhibitor, depsipeptide (FR901228, NSC 630176), in patients with refractory neoplasms. *Clin Cancer Res* 8:718–28

Sato A, Ohtsuki M, Hata M, Kobayashi E, Murakami T (2006) Antitumor activity of IFN-lambda in murine tumor models. *J Immunol* 176: 7686–94

Seliger B, Maeurer MJ, Ferrone S (2000) Antigen-processing machinery breakdown and tumor growth. *Immunol Today* 21:455–64

Singh TR, Shankar S, Srivastava RK (2005) HDAC inhibitors enhance the apoptosis-inducing potential of TRAIL in breast carcinoma. *Oncogene* 24:4609–23

Stadler WM, Margolin K, Ferber S, McCulloch W, Thompson JA (2006) A phase II study of depsipeptide in refractory metastatic renal cell cancer. *Clin Genitourin Cancer* 5:57–60

Tsai V, Southwood S, Sidney J, Sakaguchi K, Kawakami Y, Appella E *et al.* (1997) Identification of subdominant CTL epitopes of the GP100 melanoma-associated tumor antigen by primary *in vitro* immunization with peptide-pulsed dendritic cells. *J Immunol* 158: 1796–802

Ueda H, Manda T, Matsumoto S, Mukumoto S, Nishigaki F, Kawamura I *et al.* (1994a) FR901228, a novel antitumor bicyclic depsipeptide produced by Chromobacterium violaceum No. 968. III. Antitumor activities on experimental tumors in mice. *J Antibiot (Tokyo)* 47: 315–23

Ueda H, Nakajima H, Hori Y, Goto T, Okuhara M (1994b) Action of FR901228, a novel antitumor bicyclic depsipeptide produced by Chromobacterium violaceum no. 968, on Ha-ras transformed NIH3T3 cells. *Biosci Biotechnol Biochem* 58:1579–83

Williams A, Peh CA, Elliott T (2002) The cell biology of MHC class I antigen presentation. *Tissue Antigens* 59:3–17

Zlotnik A (2006) Chemokines and cancer. *Int J Cancer* 119:2026–9

Synergistic antitumor activity of the novel SN-38-incorporating polymeric micelles, NK012, combined with 5-fluorouracil in a mouse model of colorectal cancer, as compared with that of irinotecan plus 5-fluorouracil

Takako Eguchi Nakajima[1,2], Masahiro Yasunaga[2], Yasuhiko Kano[3], Fumiaki Koizumi[4], Ken Kato[1], Tetsuya Hamaguchi[1], Yasuhide Yamada[1], Kuniaki Shirao[1], Yasuhiro Shimada[1] and Yasuhiro Matsumura[2*]

[1]*Gastrointestinal Oncology Division, National Cancer Center Hospital, Tokyo, Japan*
[2]*Investigative Treatment Division, Research Center for Innovative Oncology, National Cancer Center Hospital East, Kashiwa, Chiba, Japan*
[3]*Hematology Oncology, Tochigi Cancer Center, Tochigi, Japan*
[4]*Shien Lab Medical Oncology Division, National Cancer Center Hospital, Tokyo, Japan*

Int. J. Cancer: **122,** 2148–2153 (2008)

Synergistic antitumor activity of the novel SN-38-incorporating polymeric micelles, NK012, combined with 5-fluorouracil in a mouse model of colorectal cancer, as compared with that of irinotecan plus 5-fluorouracil

Takako Eguchi Nakajima[1,2], Masahiro Yasunaga[2], Yasuhiko Kano[3], Fumiaki Koizumi[4], Ken Kato[1], Tetsuya Hamaguchi[1], Yasuhide Yamada[1], Kuniaki Shirao[1], Yasuhiro Shimada[1] and Yasuhiro Matsumura[2]*

[1]*Gastrointestinal Oncology Division, National Cancer Center Hospital, Tokyo, Japan*
[2]*Investigative Treatment Division, Research Center for Innovative Oncology, National Cancer Center Hospital East, Kashiwa, Chiba, Japan*
[3]*Hematology Oncology, Tochigi Cancer Center, Tochigi, Japan*
[4]*Shien Lab Medical Oncology Division, National Cancer Center Hospital, Tokyo, Japan*

The authors reported in a previous study that NK012, a 7-ethyl-10-hydroxy-camptothecin (SN-38)-releasing nano-system, exhibited high antitumor activity against human colorectal cancer xenografts. This study was conducted to investigate the advantages of NK012 over irinotecan hydrochloride (CPT-11) administered in combination with 5-fluorouracil (5FU). The cytotoxic effects of NK012 or SN-38 (an active metabolite of CPT-11) administered in combination with 5FU was evaluated *in vitro* in the human colorectal cancer cell line HT-29 by the combination index method. The effects of the same drug combinations was also evaluated *in vivo* using mice bearing HT-29 and HCT-116 cells. All the drugs were administered i.v. 3 times a week; NK012 (10 mg/kg) or CPT11 (50 mg/kg) was given 24 hr before 5FU (50 mg/kg). Cell cycle analysis in the HT-29 tumors administered NK012 or CPT-11 *in vivo* was performed by flow cytometry. NK012 exerted more synergistic activity with 5FU compared to SN-38. The therapeutic effect of NK012/5FU was significantly superior to that of CPT-11/5FU against HT-29 tumors ($p = 0.0004$), whereas no significant difference in the antitumor effect against HCT-116 tumors was observed between the 2-drug combinations ($p = 0.2230$). Cell-cycle analysis showed that both NK012 and CPT-11 tend to cause accumulation of cells in the S phase, although this effect was more pronounced and maintained for a more prolonged period with NK012 than with CPT-11. Optimal therapeutic synergy was observed between NK012 and 5FU, therefore, this regimen is considered to hold promise of clinical benefit, especially for patients with colorectal cancer.

Key words: NK012; SN-38; 5-fluorouracil; drug delivery system; colorectal cancer

The 5-year survival rates of colorectal cancer (CRC) have improved remarkably over the last 10 years, accounted for in large part by the extensively investigated agents after 5-fluorouracil (5FU). Irinoetcan hydrochloride (CPT-11), a water-soluble, semi-synthetic derivative of camptothecin, is one such agent that has been shown to be highly effective, and currently represents a key-drug in first- and second-line treatment regimens for CRC. CPT-11 monotherapy, however, has not been shown to yield superior efficacy, including in terms of the median survival time, to bolus 5FU/leucovorin (LV) alone.[1] In 2 Phase III trials, the addition of CPT-11 to bolus or infusional 5FU/LV regimens clearly yielded greater efficacy than administration of 5FU/LV alone, with a doubling of the tumor response rate and prolongation of the median survival time by 2–3 months.[1,2]

CPT-11 is converted to 7-ethyl-10-hydroxy-camptothecin (SN-38), a biologically active and water-insoluble metabolite of CPT-11, by carboxylesterases in the liver and the tumor. SN-38 has been demonstrated to exhibit up to a 1,000-fold more potent cytotoxic activity than CPT-11 against various cancer cells *in vitro*.[3] The metabolic conversion rate is, however, very low, with only <10% of the original volume of CPT-11 being metabolized to SN-38[4,5]; conversion of CPT-11 to SN-38 also depends on genetic interindividual variability of the activity of carboxylesterases.[6] Direct use of SN-38 itself for clinical cancer treatment must be shown to be identical in terms of both efficacy and toxicity.

Some drugs incorporated in drug delivery systems (DDS), such as Abraxane and Doxil, are already in clinical use.[7,8] The clinical benefits of DDS are based on their EPR effect.[9] The EPR effect is based on the pathophysiological characteristics of solid tumor tissues: hypervascularity, incomplete vascular architecture, secretion of vascular permeability factors stimulating extravasation within cancer tissue, and absence of effective lymphatic drainage from the tumors that impedes the efficient clearance of macromolecules accumulated in solid tumor tissues. Several types of DDS can be used for incorporation of a drug. A liposome-based formulation of SN-38 (LE-SN38) has been developed, and a clinical trial to assess its efficacy is now under way.[10,11]

Recently, we demonstrated that NK012, novel SN-38-incorporating polymeric micelles, exerted superior antitumor activity and less toxicity than CPT-11.[12] NK012 is characterized by a smaller size of the particles than LE-SN38; the mean particle diameter of NK012 is 20 nm. NK012 can release SN-38 under neutral conditions even in the absence of a hydrolytic enzyme, because the bond between SN-38 and the block copolymer is a phenol ester bond, which is stable under acidic conditions and labile under mild alkaline conditions. The release rate of SN-38 from NK012 under physiological conditions is quite high; more than 70% of SN-38 is released within 48 hr. We speculated that the use of NK012, in place of CPT-11, in combination with 5FU may yield superior results in the treatment of CRC. In the present study, we evaluated the antitumor activity of NK012 administered in combination with 5FU as compared to that of CPT-11 administered in combination with 5FU against CRC in an experimental model.

Material and methods

Cells and animals

The human colorectal cancer cell lines used, namely, HT-29 and HCT-116, were purchased from the American Type Culture Collection (Rockville, MD). The HT-29 cells and HCT-116 cells were maintained in RPMI 1640 supplemented with 10% fetal bovine serum (Cell Culture Technologies, Gaggenau-Hoerden, Germany), penicillin, streptomycin, and amphotericin B (100 units/mL, 100 μg/mL, and 25 μg/mL, respectively; Sigma, St. Louis, MO) in a humidified atmosphere containing 5% CO_2 at 37°C.

BALB/c *nu/nu* mice were purchased from SLC Japan (Shizuoka, Japan). Six-week-old mice were subcutaneously (s.c.)

***Correspondence to:** Investigative Treatment Division, Research Center for Innovative Oncology, National Cancer Center Hospital East, 6-5-1 Kashiwanoha, Kashiwa, Chiba 277-8577, Japan. Fax: +81-4-7134-6866.
E-mail: yhmatsum@east.ncc.go.jp
Received 2 September 2007; Accepted after revision 20 November 2007
DOI 10.1002/ijc.23381
Published online 14 January 2008 in Wiley InterScience (www.interscience.wiley.com).

inoculated with 1×10^6 cells of HT-29 or HCT-116 cell line in the flank region. The length (a) and width (b) of the tumor masses were measured twice a week, and the tumor volume (TV) was calculated as follows: $TV = (a \times b^2)/2$. All animal procedures were performed in compliance with the Guidelines for the Care and Use of Experimental Animals established by the Committee for Animal Experimentation of the National Cancer Center; these guidelines meet the ethical standards required by law and also comply with the guidelines for the use of experimental animals in Japan.

Drugs

The SN-38-incorporating polymeric micelles, NK012, and SN-38 were prepared by Nippon Kayaku (Tokyo, Japan).[12] CPT-11 was purchased from Yakult Honsha (Tokyo, Japan). 5FU was purchased from Kyowa Hakko (Tokyo, Japan).

Cell growth inhibition assay

HT-29 cells were seeded in 96-well plates at a density of 2,000 cells/well in a final volume of 90 μL. Twenty-four hours after seeding, a graded concentration of NK012 or SN-38 was added concurrently with 5FU to the culture medium of the HT-29 cells in a final volume of 100 μL for drug interaction studies. The culture was maintained in the CO_2 incubator for an additional 72 hr. Then, cell growth inhibition was measured by the tetrazolium salt-based proliferation assay (WST assay; Wako Chemicals, Osaka, Japan). WST-1 labeling solution (10 μL) was added to each well and the plates were incubated at 37°C for 3 hr. The absorbance of the formazan product formed was detected at 450 nm in a 96-well spectrophotometric plate reader. Cell viability was measured and compared to that of the control cells. Each experiment was carried out in triplicate and was repeated at least 3 times. Data were averaged and normalized against the nontreated controls to generate dose-response curves.

Drug interaction analysis

The nature of interaction between NK012 or SN-38 and 5FU against HT-29 cells was evaluated by median-effect plot analyses and the combination index (CI) method of Chou and Talalay.[13] Data analysis was performed using the Calcusyn software (Biosoft, NY, USA). NK012 or SN-38 was combined with 5FU at a fixed ratio that spanned the individual IC_{50} values of each drug. The IC_{50} values were determined on the basis of the dose-response curves using the WST assay. For any given drug combination, the CI is known to represent the degree of synergy, additivity or antagonism. It is expressed in terms of fraction-affected (*Fa*) values, which represents the percentage of cells killed or inhibited by the drug. Isobologram equations and *Fa*/CI plots were constructed by computer analysis of the data generated from the median effect analysis. Each experiment was performed in triplicate with 6 gradations and was repeated at least 3 times. The resultant dose-response curves were averaged, to create a single composite dose-response curve for each combination.

In vivo analysis of the effects of NK012 combined with 5FU as compared to those of CPT-11 combined with 5FU

When the mean tumor volumes reached ~93 mm^3, the mice were randomly divided into test groups consisting of 5 mice per group (Day 0). The drugs were administered i.v. *via* the tail vein of the mice. In the groups administered NK012 or 5FU as single agents, the drug was administered on Days 0, 7 and 14. In the combined treatment groups, NK012 or CPT-11 was administered 24 hr before 5FU on Days 0, 7 and 14, according to the previously reported combination schedule for CPT-11 and 5FU.[14] Complete response (CR) was defined as tumor not detectable by palpation at 90 days after the start of treatment, at which time-point the mice were sacrificed. Tumor volume and body weight were measured twice a week. As a general rule, animals in which the tumor volume exceeded 2,000 mm^3 were also sacrificed.

Experiment 1. Evaluation of the effects of NK012 combined with 5FU and determination of the maximum tolerated dose (MTD) of NK012/5FU. By comparing the data between NK012 administered as a single agent and NK012/5FU, we evaluated the effects of the combined regimen against the s.c HT-29 tumors. A preliminary experiment showed that combined administration of NK012 15 mg/kg + 5FU 50 mg/kg every 6 days caused drug-related lethality (data not shown). To determine the MTD, therefore, we set the dosing schedule of the combined regimen at 5 or 10 mg/kg of NK012 + 50 mg/kg of 5FU three times a week.

Experiment 2. Comparison of the antitumor effect of NK012/5FU and CPT-11/5FU. Based on a comparison of the data between NK012/5FU and CPT-11/5FU against the s.c. HT-29 and HCT-116 tumors, we investigated the feasibility of the clinical application of NK012/5FU for the treatment of CRC. CPT-11/5FU was administered three times a week at the respective MTDs of the 2 drugs as previously reported, that is, CPT11 at 50 mg/kg and 5FU at 50 mg/kg, respectively.[14] NK012/5FU was administered once three times a week at the respective MTDs of the 2 drugs determined from Experiment 1.

Cell cycle analysis

Samples from the HT-29 tumors that had grown to 80–100 mm^3 were removed from the mice at 6, 24, 48, 72 and 96 hr after the administration of NK012 alone at 10 mg/kg or CPT-11 alone at 50 mg/kg. The samples were excised, minced in PBS and fixed in 70% ethanol at −20°C for 48 hr. They were then digested with 0.04% pepsin (Sigma chemical Co., St Lous, MO) in 0.1 N HCL for 60 min at 37°C in a shaking bath to prepare single-nuclei suspensions. The nuclei were then centrifuged, washed twice with PBS and stained with 40 μg/mL of propidium iodide (Molecular Probes, OR) in the presence of 100 μg/mL RNase in 1 mL PBS for 30 min at 37°C. The stained nuclei were analyzed with B-D FACSCalibur (BD Biosciences, San Jose, CA), and the cell cycle distribution was analyzed using the Modfit program (Verity Software House Topsham, ME).

Statistical analyses

Data were expressed as mean ± SD. Data were analysed with Student's t test when the groups showed equal variances (F test), or Welch's test when they showed unequal variances (F test). $p < 0.05$ was regarded as statistically significant. All statistical tests were 2-sided.

Results

Antiproliferative effects of NK012 or SN-38 administered in combination with 5FU

Figure 1*a* shows the dose-response curves for NK012 alone, 5FU alone and a combination of the two. The IC_{50} levels of NK012 and 5FU against the HT-29 cells were 39 nM and 1 μM, respectively, and the IC_{50} level of SN-38 was 14 nM (data not shown). Based on these data, the molar ratio of NK012 or SN-38:5FU of 1:1,000 was used for the drug combination studies.

Figures 1*b* and 1*c* show the median-effect and the combination index plots. Combination indices (CIs) of <1.0 are indicative of synergistic interactions between 2 agents; additive interactions are indicated by CIs of 1.0, and antagonism by CIs of >1.0. Figure 1*c* shows the combination index for NK012 and 5FU, when 2 drugs are supposed to be mutually exclusive. Marked synergism was observed between Fa 0.2 and 0.6. Theoretically, the CI method is the most reliable around an Fa of 0.5, suggesting synergistic effects of the combination of NK012 and 5FU. This synergistic effect was more evident than that of SN-38/5FU (Fig. 1*d*).

In vivo *effect of combined NK012 and 5FU*

Experiment 1. Dose optimization and effect of combined NK012 and 5FU against HT-29 tumors. Comparison of the relative tumor volumes on Day 40 revealed significant differences between

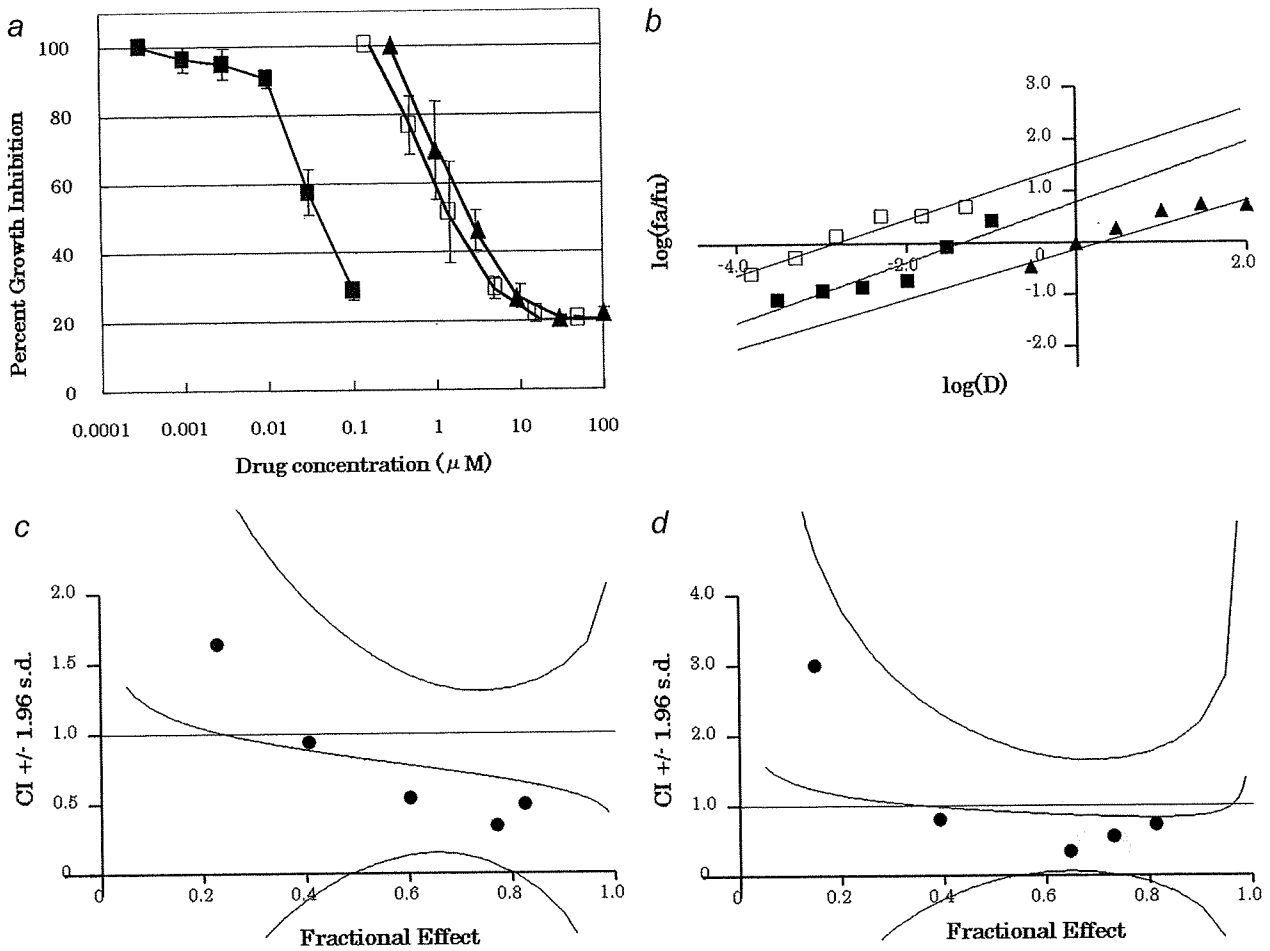

FIGURE 1 – Interaction of NK012 and 5FU *in vitro*. (*a*) Dose-response curves for NK012 alone (■), 5FU alone (▲) and their combination (□) against HT-29 cells. HT-29 cells were seeded at 2,000 cells/well. Twenty-four hours after seeding, a graded concentration of NK012 or 5FU was added to the culture medium of the HT-29 cells. Cell growth inhibition was measured by WST assay after 72 hr of treatment. Cell viability was measured and compared with that of the control cells. Each experiment was carried out independently and repeated at least 3 times. Points, mean of tripricates; bars, SD. (*b*) Median effect plot for the interaction of NK012 and 5FU. (*c*, *d*) Combination index for the interaction as a function of the level of effect (fraction effect = 0.5 is the IC_{50}). The straight line across the CI value of 1.0 indicates additive effect and CIs above and below indicate antagonism and synergism, respectively. The molar ratio of NK012/5FU (*c*) or SN-38/5FU (*d*) at 1:1,000 was tested by CI analysis. Black circles represent the CIs of the actual data points, solid lines represent the computer-derived CIs at effect levels ranging from 10 to 100% inhibition of cell growth, and the dotted lines represent the 95% confidence intervals.

those in the mice administered NK012 alone and those administered NK012/5FU at 5 mg/kg of NK012 ($p = 0.018$) (Fig. 2*a*). Although there was no statistically significant difference in the relative tumor volume measured on Day 54 between the mice administered NK012 alone and NK012/5FU at 10 mg/kg of NK012 ($p = 0.3050$), a trend of superior antitumor effect was demonstrated in the group treated with NK012/5FU at 10 mg/kg of NK012 (Fig. 2*a*). The CR rates were 20, 40 and 60% for 5 mg/kg NK012 + 50 mg/kg 5FU, 10 mg/kg NK012 alone and 10 mg/kg NK012 + 50 mg/kg 5FU, respectively. The schedule of 10 mg/kg NK012 + 50 mg/kg 5FU resulted in no remarkable toxicity in terms of body weight changes, and these doses were determined as representing the MTDs (Fig. 2*b*).

Experiment 2. Comparison of the antitumor effect of combined NK012/5FU and CPT-11/5FU against HT-29 and HCT-116 tumors. The therapeutic effect of NK012/5FU on Day 60 was significantly superior to that of CPT-11/5FU against the HT-29 tumors ($p = 0.0004$) (Fig. 3*a*). A more potent antitumor effect, namely, a 100% CR rate, was obtained in the NK012/5FU group as compared to the 0% CR rate in the CPT-11/5FU group. Although no statistically significant difference in the relative tumor volume on Day 61 was demonstrated between the NK012/5FU and CPT-11/5FU in the case of the HCT-116 tumors ($p = 0.2230$), a trend of superior antitumor effect against these tumors was observed in the NK012/5FU treatment group (Fig. 3*b*). The CR rates for the case of the HCT-116 tumors were 0% in both NK012/5FU and CPT-11/5FU groups.

Specificity of cell cycle perturbation

We studied the differences in the effects between NK012 10 mg/kg and CPT-11 50 mg/kg on the cell cycle (Fig. 4*a*). The data indicated that both NK012 and CPT-11 tended to cause accumulation of cells in the S phase, although the effect of NK012 was stronger and maintained for a more prolonged period than that of CPT-11; the maximal percentage of S-phase cells in the total cell population in the tumors was 34% at 24 hr after the administration of CPT-11, whereas it was 39% at 48 hr after the administration of NK012 (Figs. 4*b*, and 4*c*).

Discussion

Our primary endpoint was to clarify the advantages of NK012 over CPT-11 administered in combination with 5FU. We demonstrated that combined NK012 and 5FU chemotherapy exerts more

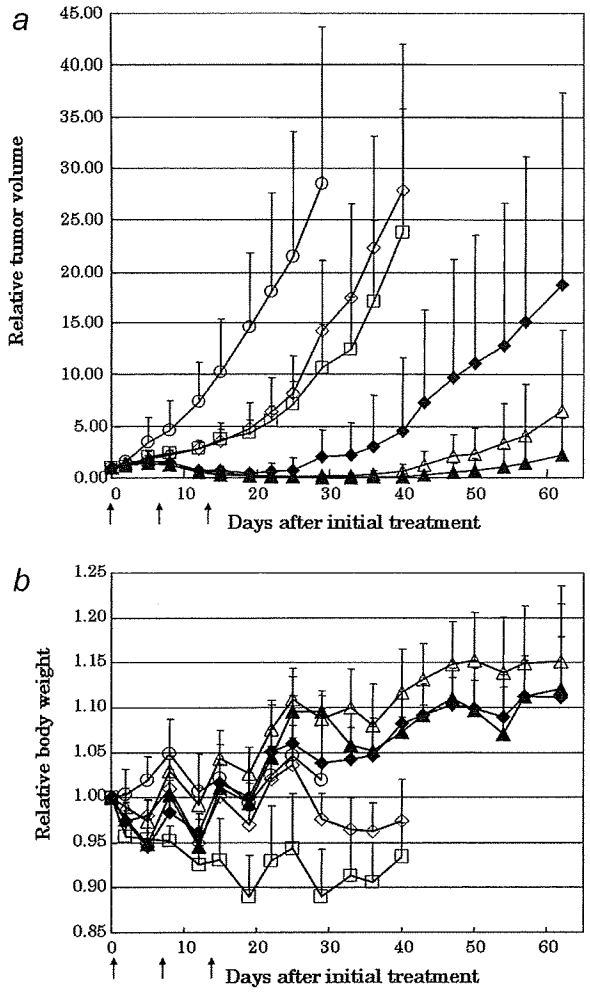

FIGURE 2 – Effect of NK012 alone or NK012 in combination with 5FU against HT-29 tumor-bearing mice. Points, mean; bars, SD. (*a*) Antitumor effect of each regimen on Days 0, 7 and 14. (○) control, (□) 5FU 50 mg/kg alone, (◇) NK012 5 mg/kg alone, (◆) NK012 5 mg/kg 24 hr before 5FU 50 mg/kg, (△) NK012 10 mg/kg alone, (▲) NK012 10 mg/kg 24 hr before 5FU 50 mg/kg. (*b*) Changes in the relative body weight. Data were derived from the same mice as those used in the present study.

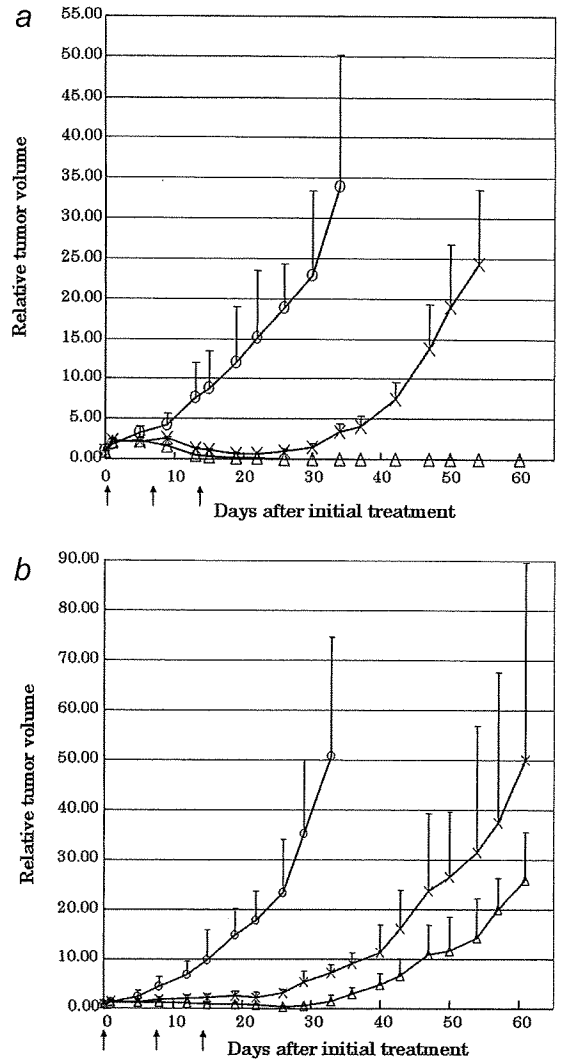

FIGURE 3 – Effect of NK012/5FU as compared with that of CPT11/5FU against HT-29 (*a*) or HCT-116 (*b*) tumor-bearing mice. Antitumor effect of each schedule on Days 0, 7 and 14. (○) control, (×) CPT-11 50 mg/kg 24 hr before 5FU 50 mg/kg, (△) NK012 10 mg/kg 24 hr before 5FU 50 mg/kg. Points, mean; bars, SD.

synergistic activity *in vitro* and significantly greater antitumor activity against human CRC xenografts as compared to CPT-11/5FU. The combination of NK012 and 5FU is considered to hold promise of clinical benefit for patients with CRC.

CPT-11, a topoisomerase-I inhibitor, and 5FU, a thymidilate synthase inhibitor, have been demonstrated to be effective agents for the treatment of CRC. A combination of these 2 drugs has also been demonstrated to be clearly more effective than either CPT-11 or 5FU/LV administered alone *in vivo* and in clinical settings.[1,2,14] Administration of 5FU by infusion with CPT-11 was shown to be associated with reduced toxicity and an apparent improvement in survival as compared to that of administration of the drug by bolus injection with CPT-11.[1,2] This synergistic enhancement may result from the mechanism of action of the 2 drugs; CPT-11 has been reported to cause accumulation of cells in the S phase, and 5FU infusion is known to cause DNA damage specifically in cells of the S phase.[14] On the basis of this background, our results suggesting the more pronounced and more prolonged accumulation of the tumor cells in the S phase caused by NK012 as compared with that by CPT-11 may explain the more effective synergy of the former administered with 5FU infusion. This may be attributable to accumulation of NK012 due to the enhanced permeability and retention (EPR) effect.[9] It is also speculated that NK012 allows sustained release of free SN-38, which may move more freely in the tumor interstitium.[15] Otherwise NK012 itself could internalize into cells to localize in several cytoplasmic organelles as reported by Savic *et al.*[16] These characteristics of NK012 may be responsible for its more potent antitumor activity observed in this study, because CPT-11 has been reported to show time-dependent growth-inhibitory activity against the tumor cells.[17]

The major dose-limiting toxicities of CPT-11 are diarrhea and neutropenia. SN-38, the active metabolite of CPT-11, may cause CPT-11-related diarrhea as a result of mitotic -inhibitory activity.[18] Because it undergoes significant biliary excretion, SN-38 may have a potentially long residence time in the gastrointestinal tract that may be associated with prolonged diarrhea.[19,20] In our previous report, we evaluated the tissue distribution of SN-38 after administration of an equimolar amount of NK012 (20 mg/kg) and CPT-11 (30 mg/kg), and found no difference in the level of SN-38 accumulation in the small intestine.[12] A significant antitumor effect of NK012 with a lower incidence of diarrhea was also dem-

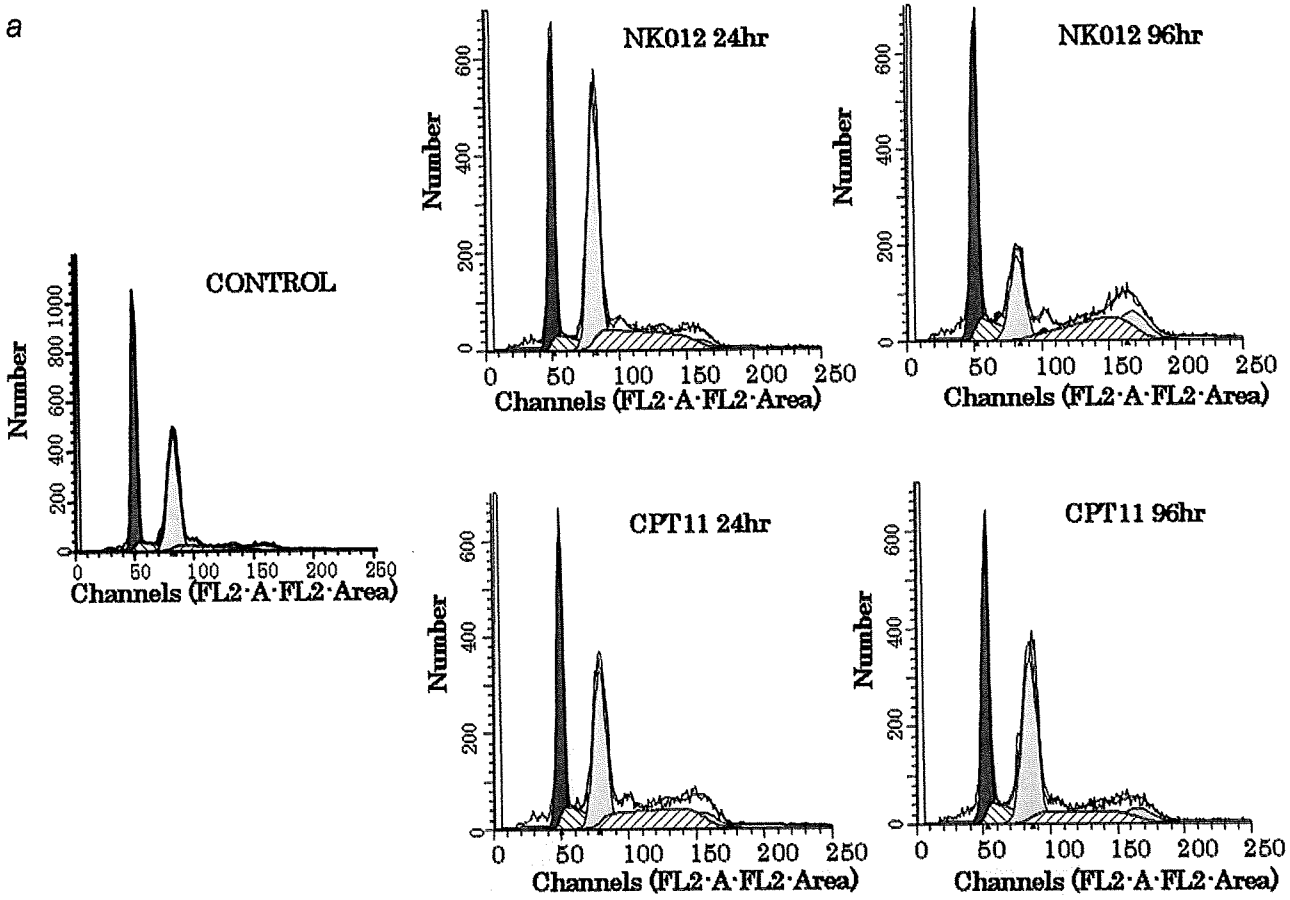

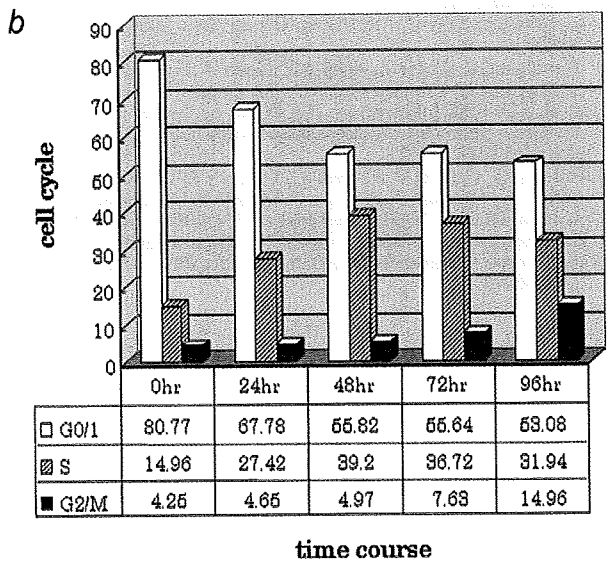

	0hr	24hr	48hr	72hr	96hr
□ G0/1	80.77	67.78	55.82	55.64	53.08
▨ S	14.96	27.42	39.2	36.72	31.94
■ G2/M	4.25	4.65	4.97	7.63	14.96

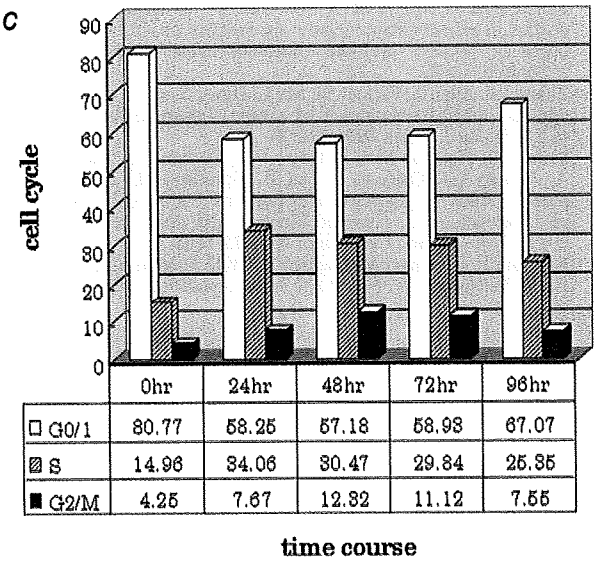

	0hr	24hr	48hr	72hr	96hr
□ G0/1	80.77	58.25	57.18	58.93	67.07
▨ S	14.96	34.06	30.47	29.84	25.35
■ G2/M	4.25	7.67	12.32	11.12	7.55

FIGURE 4 – Cell cycle analysis of HT-29 tumor cells collected 24, 48, 72 and 96 hr after administration of NK012 at 10 mg/kg alone or CPT-11 at 50 mg/kg alone using the Modfit program (Verity Software House Topsham, ME). (*a*) Cell cycle analysis of HT-29 tumor cells 24 and 96 hr after administration of NK012 at 10 mg/kg or CPT-11 at 50 mg/kg, respectively. (*b*) Cell cycle distribution of tumor cells 0, 24, 48, 72 and 96 hr after treatment with NK012 at 10 mg/kg. (*c*) Cell cycle distribution of tumor cells 0, 24, 48, 72 and 96 hr after treatment with CPT-11 at 50 mg/kg.

onstrated as compared to that observed with CPT-11 in a rat mammary tumor model.[21] Combined administration of CPT-11 with 5FU/LV infusion appears to be associated with acceptable toxicity in patients with CRC. In addition, no significant difference in the frequency of Grade 3/4 diarrhea was noted between patients treated with FOLFIRI (CPT-11 regimen with bolus and infusional 5FU/LV) and those treated with FOLFOX6 (oxaliplatin regimen with bolus and infusional 5FU/LV).[22,23] Our *in vivo* data actually revealed no severe body weight loss in the NK012/5FU group. Consequently, we expect that the NK012/5FU regimen, especially

with infusional 5FU, may be an attractive arm for a Phase III trial in CRC, with CPT-11/5FU as the control arm. We have already initiated a Phase I trial of NK012 in patients with advanced solid tumors based on the data suggesting higher efficacy and lower toxicity of this preparation than CPT-11 *in vivo*.[12]

In conclusion, we demonstrated that combined NK012 and 5FU chemotherapy exerts significantly greater antitumor activity against human CRC xenografts as compared to CPT-11/5FU, indicating the necessity of clinical evaluation of this combined regimen.

References

1. Saltz LB, Douillard JY, Pirotta N, Alakl M, Gruia G, Awad L, Elfring GL, Locker PK, Miller LL. Irinotecan plus fluorouracil/leucovorin for metastatic colorectal cancer: a new survival standard. Oncologist 2001;6:81–91.
2. Douillard JY, Cunningham D, Roth AD, Navarro M, James RD, Karasek P, Jandik P, Iveson T, Carmichael J, Alakl M, Gruia G, Awad L, et al. Irinotecan combined with fluorouracil compared with fluorouracil alone as first-line treatment for metastatic colorectal cancer: a multicentre randomised trial. Lancet 2000;355:1041–7.
3. Takimoto CH, Arbuck SG. Topoisomerase I targeting agents: the camptothecins. In: Chabner BA, Lango DL, eds. Cancer chemotherapy and biotherapy: principal and practice, 3rd ed. Philadelphia, PA: Lippincott Williams and Wilkins, 2001. 579–646.
4. Slatter JG, Schaaf LJ, Sams JP, Feenstra KL, Johnson MG, Bombardt PA, Cathcart KS, Verburg MT, Pearson LK, Compton LD, Miller LL, Baker DS, et al. Pharmacokinetics, metabolism, and excretion of irinotecan (CPT-11) following I.V. infusion of [(14)C]CPT-11 in cancer patients. Drug Metab Dispos 2000;28:423–33.
5. Rothenberg ML, Kuhn JG, Burris HA, III, Nelson J, Eckardt JR, Tristan-Morales M, Hilsenbeck SG, Weiss GR, Smith LS, Rodriguez GI, Rock MK, Von Hoff DD. Phase I and pharmacokinetic trial of weekly CPT-11. J Clin Oncol 1993;11:2194–204.
6. Guichard S, Terret C, Hennebelle I, Lochon I, Chevreau P, Fretigny E, Selves J, Chatelut E, Bugat R, Canal P. CPT-11 converting carboxylesterase and topoisomerase activities in tumour and normal colon and liver tissues. Br J Cancer 1999;80:364–70.
7. Gradishar WJ, Tjulandin S, Davidson N, Shaw H, Desai N, Bhar P, Hawkins M, O'Shaughnessy J. Phase III trial of nanoparticle albumin-bound paclitaxel compared with polyethylated castor oil-based paclitaxel in women with breast cancer. J Clin Oncol 2005;23:7794–803.
8. Muggia FM. Liposomal encapsulated anthracyclines: new therapeutic horizons. Curr Oncol Rep 2001;3:156–62.
9. Matsumura Y, Maeda H. A new concept for macromolecular therapeutics in cancer chemotherapy: mechanism of tumoritropic accumulation of proteins and the antitumor agent smancs. Cancer Res 1986;46:6387–92.
10. Zhang JA, Xuan T, Parmar M, Ma L, Ugwu S, Ali S, Ahmad I. Development and characterization of a novel liposome-based formulation of SN-38. Int J Pharm 2004;270:93–107.
11. Kraut EH, Fishman MN, LoRusso PM, Gorden MS, Rubin EH, Haas A, Fetterly GJ, Cullinan P, Dul JL, Steinberg JL. Final result of a phase I study of liposome encapsulated SN-38 (LE-SN38): safety, pharmacogenomics, pharmacokinetics, and tumor response [abstract 2017]. Proc Am Soc Clin Oncol 2005;23:139S.
12. Koizumi F, Kitagawa M, Negishi T, Onda T, Matsumoto S, Hamaguchi T, Matsumura Y. Novel SN-38-incorporating polymeric micelles, NK012, eradicate vascular endothelial growth factor-secreting bulky tumors. Cancer Res 2006;66:10048–56.
13. Chou TC, Talalay P. Quantitative analysis of dose-effect relationships: the combined effects of multiple drugs or enzyme inhibitors. Adv Enzyme Regul 1984;22:27–55.
14. Azrak RG, Cao S, Slocum HK, Toth K, Durrani FA, Yin MB, Pendyala L, Zhang W, McLeod HL, Rustum YM. Therapeutic synergy between irinotecan and 5-fluorouracil against human tumor xenografts. Clin Cancer Res 2004;10:1121–9.
15. Jain RK. Barriers to drug delivery in solid tumors. Sci Am 1994; 271:58–65.
16. Savic R, Luo L, Eisenberg A, Maysinger D. Micellar nanocontainers distribute to defined cytoplasmic organelles. Science 2003;300:615–18.
17. Kawato Y, Aonuma M, Hirota Y, Kuga H, Sato K. Intracellular roles of SN-38, a metabolite of the camptothecin derivative CPT-11, in the antitumor effect of CPT-11. Cancer Res 1991;51:4187–91.
18. Slater R, Radstone D, Matthews L, McDaid J, Majeed A. Hepatic resection for colorectal liver metastasis after downstaging with irinotecan improves survival. Proc Am Soc Clin Oncol 2003;22(abstract 1287).
19. Araki E, Ishikawa M, Iigo M, Koide T, Itabashi M, Hoshi A. Relationship between development of diarrhea and the concentration of SN-38, an active metabolite of CPT-11, in the intestine and the blood plasma of athymic mice following intraperitoneal administration of CPT-11. Jpn J Cancer Res 1993;84:697–702.
20. Atsumi R, Suzuki W, Hakusui H. Identification of the metabolites of irinotecan, a new derivative of camptothecin, in rat bile and its biliary excretion. Xenobiotica 1991;21:1159–69.
21. Onda T, Nakamura I, Seno C, Matsumoto S, Kitagawa M, Okamoto K, Nishikawa K, Suzuki M. Superior antitumor activity of NK012, 7-ethyl-10-hydroxycamptoyhecin-incorporating micellar nanoparticle, to irrinotecan. Proc Am Assoc Cancer Res 2006;47:720s(abstract 3062).
22. Tournigand C, Andre T, Achille E, Lledo G, Flesh M, Mery-Mignard D, Quinaux E, Couteau C, Buyse M, Ganem G, Landi B, Colin P, et al. FOLFIRI followed by FOLFOX6 or the reverse sequence in advanced colorectal cancer: a randomized GERCOR study. J Clin Oncol 2004;22:229–37.
23. Colucci G, Gebbia V, Paoletti G, Giuliani F, Caruso M, Gebbia N, Carteni G, Agostara B, Pezzella G, Manzione L, Borsellino N, Misino A, et al. Phase III randomized trial of FOLFIRI versus FOLFOX4 in the treatment of advanced colorectal cancer: a multicenter study of the Gruppo Oncologico Dell'Italia Meridionale. J Clin Oncol 2005; 23:4866–75.

Oncology Research, Vol. 17, pp. 137–149

0965-0407/08 $90.00 + .00
E-ISSN 1555-3906
www.cognizantcommunication.com

Long-Term Results of Dose-Intensive Chemotherapy With G-CSF Support (TCC-NHL-91) for Advanced Intermediate-Grade Non-Hodgkin's Lymphoma: A Review of 59 Consecutive Cases Treated at a Single Institute

Miyuki Akutsu,* Saburo Tsunoda,* Tohru Izumi,* Masaru Tanaka,* Susumu Katano,† Koichi Inoue,* Seiji Igarashi,‡ Kaoru Hirabayashi,‡ Yusuke Furukawa,§ Ken Ohmine,*§ Kazuya Sato,*§ Hiroyuki Kobayashi,*§ Keiya Ozawa,§ Keita Kirito,*¶ Takahiro Nagashima,*¶ Satoshi Teramukai,# Masanori Fukushima,# and Yasuhiko Kano*

*Division of Hematology, Tochigi Cancer Center, Tochigi, 320-0834, Japan
†Division of Radiation Oncology, Tochigi Cancer Center, Tochigi, 320-0834, Japan
‡Division of Pathology, Tochigi Cancer Center, Tochigi, 320-0834, Japan
§Division of Hematology, Jichi Medical University, Tochigi 329-0498, Japan
¶Division of Hematology, Yamanashi University, Yamanashi 409-3898, Japan
#Division of Clinical Trial Design and Management, Translational Research Center, Kyoto University Hospital, Kyoto, 606-8507, Japan

(Submitted September 25, 2007; revision received January 9, 2008; accepted January 15, 2008)

We evaluated the long-term outcome of very dose-intensive chemotherapy (TCC-NHL-91) for advanced intermediate-grade lymphoma, in which an eight-cycle regimen with 11 drugs was given with granulocyte colony-stimulating factor (G-CSF) support (total 18 weeks). Fifty-nine patients were treated during February 1, 1991 and March 31, 2001 (median age: 48 years). Forty-three patients (73%) were in a high-intermediate risk or high-risk group (HI/H) according to the age-adjusted International Prognostic Index (aa-IPI). Forty-six patients received 7 or 8 cycles of therapy. Ten of 15 patients over age 60 stopped before 7 cycles. Forty-three patients with an initial bulky mass or a residual mass received involved-field radiation. Overall, 56 patients (95%) achieved complete remission (CR). Grade 4 hematotoxicity was observed in all patients. With a median follow-up of 128 months, the 10-year overall survival (OS) and progression-free survival (PFS) rates were 76% and 61%, respectively. Neither aa-IPI risk factors nor the index itself was associated with response, OS, or PFS. One patient died of sepsis during the therapy and one died of secondary leukemia. This retrospective study suggests that the TCC-NHL-91 regimen achieves high CR, OS, and PFS in patients with advanced intermediate-grade lymphoma up to 60 years old and may be a valuable asset in the management of this disease. Further evaluation and prospective studies of the TCC-NHL-91 are warranted.

Key words: TCC-NHL-91; G-CSF; Aggressive lymphoma; CNS lymphoma

INTRODUCTION

The prognosis of non-Hodgkin's lymphoma (NHL) remains unsatisfactory in spite of significant advances in treatment. The 5-year survival rate of patients with advanced aggressive NHL is about 30–40% (1,2). Many patients die of relapsed or refractory diseases. Although second- or third-generation regimens were initially reported to improve survival (3–6), a large-scale randomized study showed that these regimens had no superiority to the standard CHOP regimen (cyclophosphamide, doxorubicin, vincristine, prednisone) (2).

Recently, a chimeric monoclonal antibody, rituximab, which targets the CD20 antigen on B cells, has been introduced for clinical use. The outcome for patients with diffuse large B-cell lymphoma (DLBCL) is significantly improved (by 10–20%) by the addition of rituximab to CHOP or other regimens (7–9). However, the prognosis is still unsatisfactory for especially high-risk patients. Patients with DLBCL classified into high-intermediate and high IPI groups (HI/H) showed a long-term chance of cure in the range of 50% (9), and the survival rate in patients with mantle cell lymphoma and T-cell lymphoma was much lower than that in advanced DLBCL. No consensus was obtained during the 1990s about using high-dose therapy as a first-line therapy for poor-risk intermediate-grade lymphoma (10). It is obvious that CHOP-based therapy is far from ideal and there

Address correspondence to Yasuhiko Kano, Divison of Hematology, Tochigi Cancer Center, Yonan 4-9-13, Utsunomiya, Tochigi, 320-0834, Japan. Tel: 011-81-28-658-5151; Fax: 011-81-28-658-5488; E-mail: ykano@tcc.pref.tochigi.jp